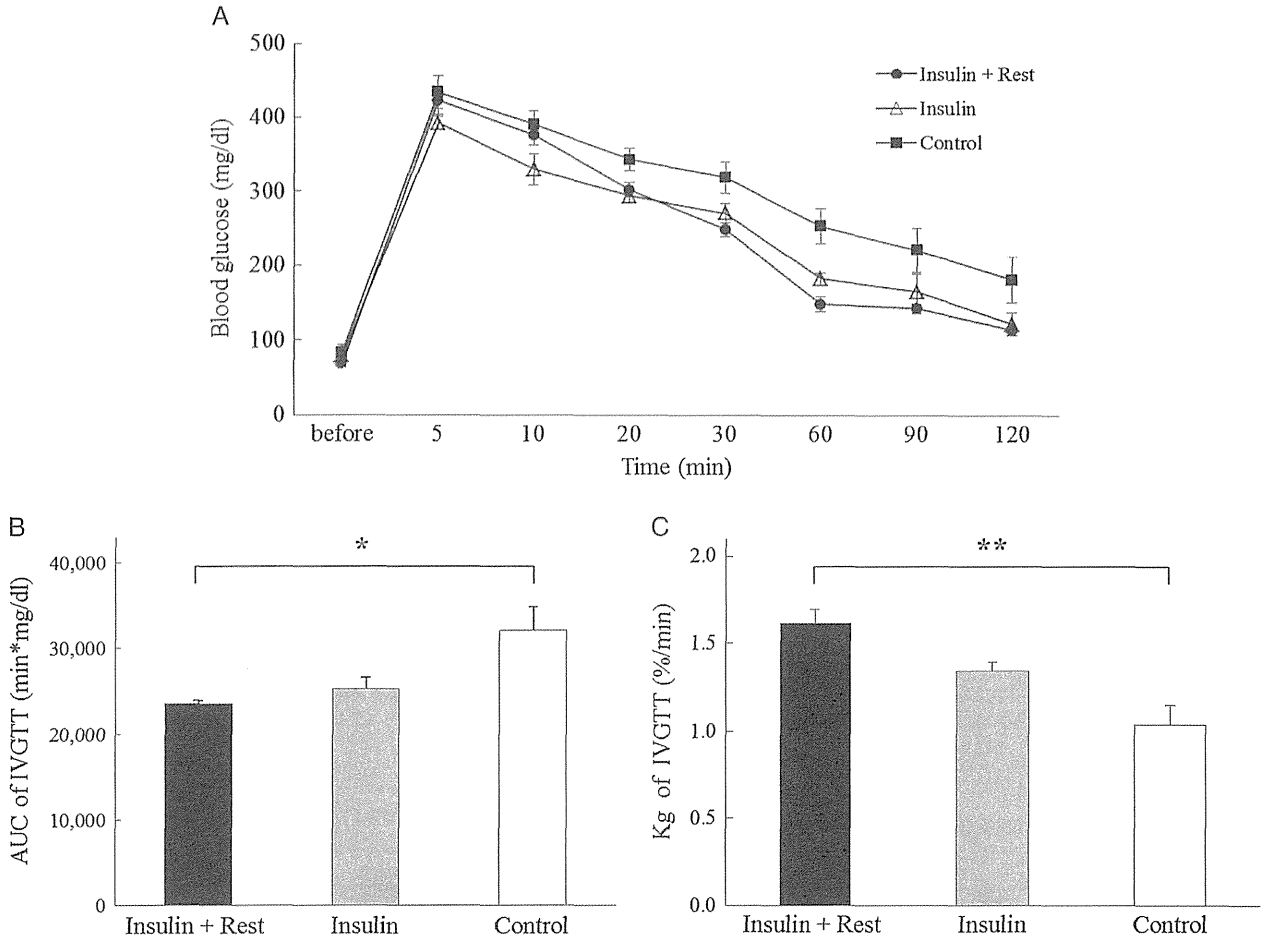

FIGURE 2. Profile of glucose tolerance in each group. A, the results of the intravenous glucose tolerance test (IVGTT) in each group at 5 weeks after transplantation. Glucose tolerance was significantly ameliorated in the insulin+rest group, but not in the insulin group, compared to the control group as indicated by both the AUC (B) (*P<0.01) and Kg values (**P<0.001) (C).

the insulin+rest group (13.2±2.3) and the insulin group (8.1±1.6) than in the control group (3.6±1.1), but the improvement was only statistically significant in the case of the insulin+rest group (P=0.002) (Fig. 3B).

The Expression of Inflammatory Mediators in Each Group

Regarding the expression of inflammatory mediators, such as TNF-α, IL-6, and MCP-1, no significant differences were observed in any of the groups on day 14 after islet transplantation (Table 1).

The Influence of Short-Term Fasting on Oxidative Stress in the Transplant Recipients

The serum levels of 8-hydroxy-2′-deoxyguanosine (8-OHdG) were measured to analyze the extent of oxidative DNA damage in each group (Table 1). Although the serum levels of 8-OHdG in the insulin+rest group were considerably lower than those of the insulin and control groups, the differences did not reach significance (P=0.08).

The Influence of Short-Term Fasting on the Glucagon-Like Peptide-1 (GLP-1) Levels

The serum active GLP-1 levels were measured in all three groups at 14 days after transplantation (Table 1). Significantly lower levels of GLP-1 were observed in the insulin+rest group compared to the insulin and the control groups (P =0.0001).

The State of Apoptosis and Revascularization of the Islet Grafts

Using the terminal deoxynucleotide transferase-mediated dUTP nick-end labeling (TUNEL) assay, the number of apoptotic islet cells in the liver sections was examined. Representative examples are shown in Figure 4A. No significant differences were observed among the groups (P=0.28) (Fig. 4C). The number of vWF-positive vessels around the islets was also counted to examine the state of revascularization of the islet grafts (Fig. 4B). The counts of the vWF-positive vessels in the insulin+rest (375±35/mm^2) and insulin groups (564±71/mm^2) were remarkably lower than those in the control group (923±227/mm^2) (P=0.08) (Fig. 4D).

DISCUSSION

A considerable number of studies to date, including a recent clinical report (*10*), have revealed that posttransplant glycemic control is crucial for successful islet transplantation (*4–9*). Most of these studies concluded that exogenous insulin treatment is beneficial to allow the transplanted islet grafts to

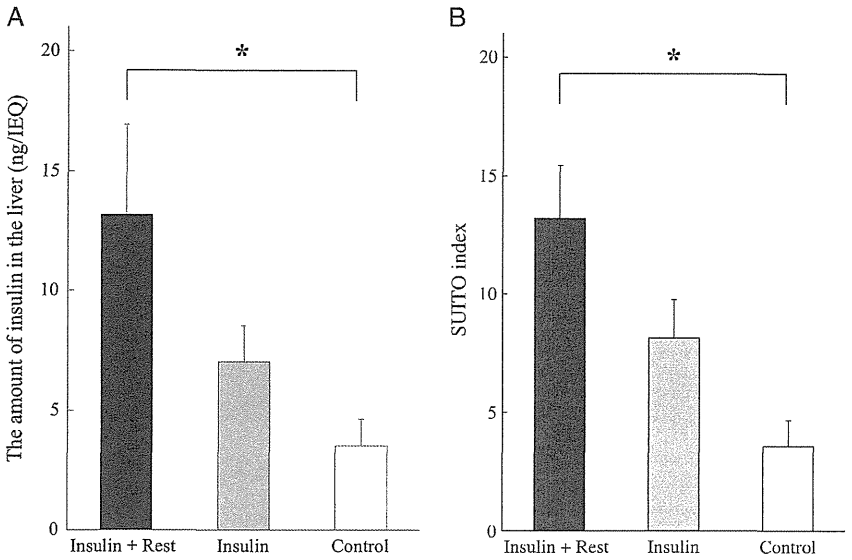

FIGURE 3. Evaluation of graft function. A, the amount of insulin in the liver. After the intravenous glucose tolerance test, the recipient livers were harvested, and the amount of insulin in the liver per transplanted islet equivalents (IEQs) was evaluated. The level was significantly higher in the insulin+rest group compared to that in the control group (*P=0.03). B, the secretory unit of islet transplant objects (SUITO) index at 5 weeks after islet transplantation. The SUITO index, which is used as an index of graft function in clinical islet transplantation, was significantly improved in the insulin+rest group compared to the control group (*P=0.002).

rest, particularly during the avascular period. Because it can minimize the workload experienced by the transplanted grafts, the regulation of postprandial hyperglycemia is therefore considered to be of great importance. However, the current manner of insulin infusion may not be sufficient to effectively prevent the development of postprandial hyperglycemia. It was therefore assumed that short-term fasting, supported by total parenteral nutrition, during a limited period after transplantation could be a helpful strategy to more effectively rest the islet grafts during the avascular period.

In the present study, normoglycemia in both the insulin+rest and insulin groups was maintained even after discontinuing insulin treatment, which did not occur in the control group. The cure rate at 5 weeks after transplantation was also significantly improved in both the insulin+rest and insulin groups compared to the control group. These results are consistent with the previous reports indicating that exogenous insulin treatment during the early stage of engraftment improved the outcome of islet transplantation (*4–10*). Furthermore, it was demonstrated that the glucose tolerance, the function of transplanted islet grafts indicated by the SUITO index (*23*), and the amount of insulin in the transplanted livers were significantly improved in the insulin+rest group, but not in the insulin group, compared to the control group. These data clearly show that short-term fasting, combined with insulin treatment during the avascular period, can better preserve transplanted islet grafts in the liver.

Although exogeneous insulin was administered subcutaneously in the previous studies (*5, 6, 12*), it was infused intravenously to more precisely control the blood glucose level in the present study. In fact, such intensive insulin treatment during the early stage of engraftment would likely be performed intravenously in the clinical setting. Moreover, in the present study, the short-term fasting was performed in conjunction with total parenteral nutrition via a central venous catheter to mimic the clinical condition. The experimental models used in the present study demonstrate approaches that could be applied clinically.

TABLE 1. The influence of short-term fasting on the expression of inflammatory mediators, oxidative stress, and glucagon-like peptide-1 (GLP-1) levels

	Insulin+rest (n=4)	Insulin (n=5)	Control (n=8)
TNFα, pg/mL	50.9±11.6	39.8±3.1	59.7±6.6
IL-6, pg/mL	3,199±752	2,651±412	4,812±933
MCP-1, pg/mL	823±182	752±53	1,018±97
8-OHdG, ng/mL	0.22±0.07	0.89±0.40	0.59±0.23
GLP-1 levels, pmol/L[a]	1.0±1.0[b] (n = 6)	9.0±1.2 (n = 6)	11.6±1.6 (n = 8)

[a] Values are obtained in the other series of experiments.
[b] P=0.0001 vs. the insulin and the control groups.
TNFα, tumor necrosis factor-alpha; IL-6, interleukin-6; MCP-1, monocyte chemoattractant protein-1; GLP-1, glucagon-like peptide-1; 8-OHdG; 8-hydroxy-2′-deoxyguanosine.
Values are means±SE.

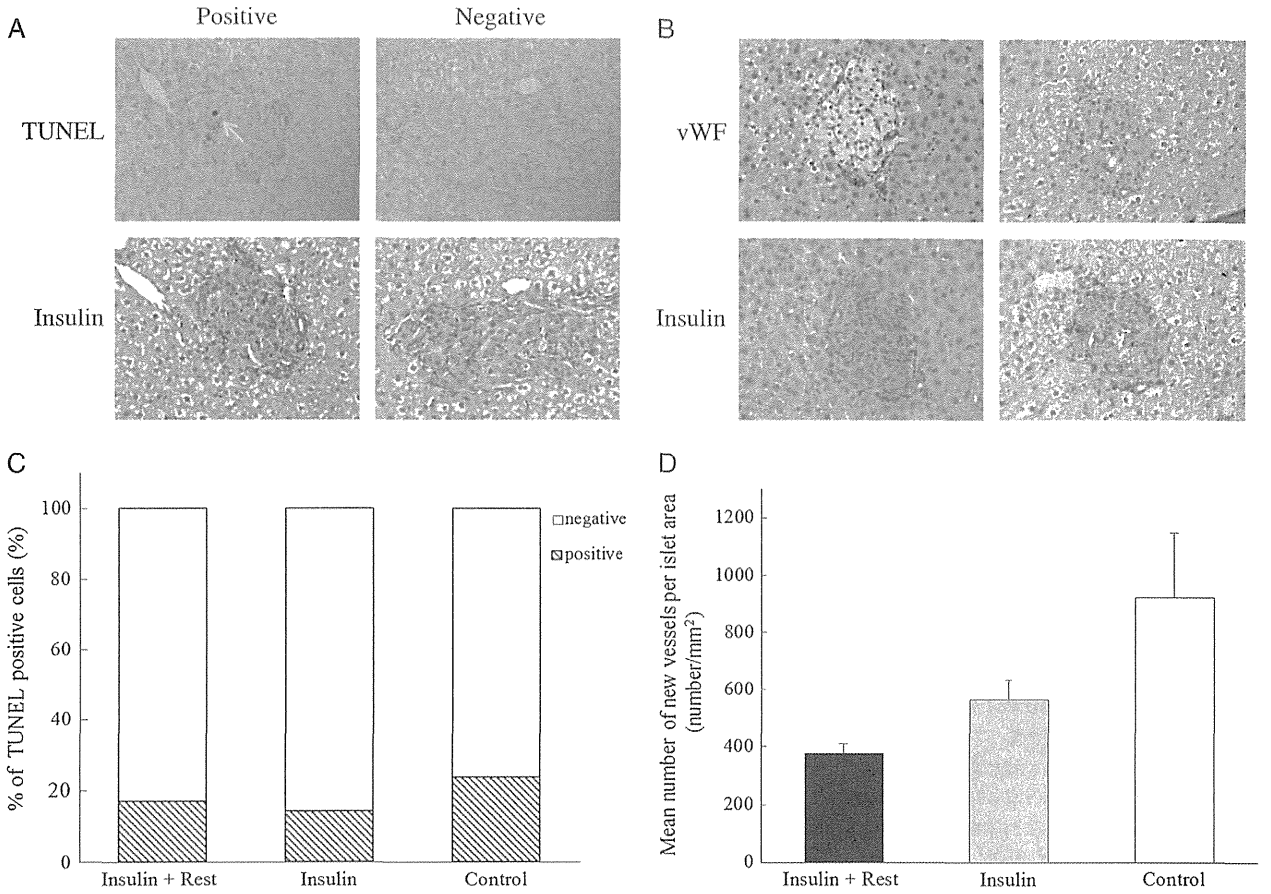

FIGURE 4. Immunohistochemical analyses. A, upper panel: TUNEL staining. Lower panel: insulin staining of the same islets. "Positive" represents TUNEL-positive cells in the islets, and "Negative" represents TUNEL-negative cells in the islets. B, upper panel: vWF staining. Lower panel: insulin staining of the same islets. C, the percentage of TUNEL-positive cells. D, Mean number of new vessels per islet area. The vWF-positive vessels in the insulin+rest (375±35/mm^2) and insulin groups (564±71/mm^2) were remarkably lower than those in the control group (923±227/mm^2) (P=0.08).

Moreover, the current rat model enabled us to achieve almost the same background, including the insulin dose, the rate of the increase in body weight, and the inflammatory status between the resting and insulin groups. Therefore, it is believed that the differences between them may be more accurately attributed to the stressful workload on the islet grafts resulting from the postprandial hyperglycemia in the non-fasting group. In this study, postprandial blood glucose fluctuation in the insulin group was not directly measured because of a technical limitation. However, postprandial hyperglycemia under continuous insulin administration has already been reported (*24, 25*) even when CSII (continuous subcutaneous insulin infusion) was introduced. Therefore, it is speculated that there was not enough regulation of postprandial hyperglycemia in the insulin group in the present study as well. Corroborating the findings of this study, Sato et al. reported that isolated islets with a high mitochondrial workload can become hypoxic, especially when the oxygen supply is limited (*22*). In that report, the authors also observed that decreasing the mitochondrial workload rescued the islet cells from becoming hypoxic. Likewise, Yanjun et al. showed that blood glucose fluctuations substantially damaged the pancreatic islets by enhancing oxidative stress (*21*). Although the difference did not reach statistical significance, it was observed that there is a tendency toward reduction of oxidative stress in the insulin+rest group in this study compared with the other groups. Because the revascularization was pronounced in the control group compared with the insulin+rest group, it seems likely that the avoidance of oxidative stress may be one of the crucial targets for preventing or overcoming islet exhaustion.

Unexpectedly, the newly formed vessels surrounding the grafts were markedly sparse in the insulin+rest and insulin groups compared with the control group. Considering that the islets subjected to the various stresses are well known to release a potent angiogenesis factor (*26*), it may be speculated that enhanced revascularization in the control group is attributed to angiogenesis factors released from the stressful islets exposed to hyperglycemia and a heavy workload. In other words, this novel finding also suggests that the grafts in the resting group appear to be free from several types of stress, and therefore the resting protocol is most likely highly effective.

In this study, both insulin treatment and fasting were performed throughout the initial 2 weeks after islet transplantation because it was previously demonstrated that the vascularization process is completed after approximately 14 days (*1, 3*). Indeed, Merino et al. reported that the beneficial effect of insulin treatment was maximal when it was maintained

throughout the 14-day revascularization period after transplantation (*5*). Considering that insulin per se seems to be a strong trophic factor for islet grafts (*19, 27–30*) and an effective inhibitor of glucotoxicity (*13–16*), it may be speculated that the optimal duration of insulin treatment would be no less than 14 days. This would be feasible in view of practical aspects as well because diabetic patients are often already being treated with insulin. On the other hand, further investigations of the optimal duration for short-term fasting are required because parenteral feeding may be associated with a risk of bacterial translocation and down-regulation of endogenous incretin production.

In the present study, the influence of short-term fasting on the serum concentration of GLP-1, one of the crucial incretins, was examined and found that the GLP-1 levels were significantly suppressed in the insulin+rest group compared to the other groups. In general, stimulation of proliferation and inhibition of the apoptosis of beta cells in vivo or in vitro studies are induced by a pharmacological level of GLP-1 analogues with a longer half-life or continuous infusion of GLP-1 (*31, 32*). Considering that the serum levels of GLP-1 in all experimental groups are within physiological level, and might not be enough to effectively circumvent apoptosis of β cells, it is believed that the advantages of graft preservation by the resting protocol outweigh the disadvantages of GLP-1 down-regulation, at least during the initial avascular period following transplantation. Of particular interest, the resting protocol, used in combination with GLP-1 analog administration, represents a promising regimen for further improving the graft function in the liver.

In summary, the present study demonstrates that short-term fasting combined with insulin treatment during the initial avascular period after transplantation could be a promising strategy for improving islet engraftment in the liver. Further optimization of the present resting protocol, especially with regard to the minimum duration of fasting, would be facilitated by a prospective clinical study.

MATERIALS AND METHODS

Animals

All animals used in the present study were handled in accordance with the Guide for the Care and Use of Laboratory Animals published by the National Institutes of Health (*33*). Male Lewis rats were used as both donors (weighing 280–350 g, 10–12 weeks of age) and recipients (weighing 220–260 g, 8 weeks of age) (Japan SLC Inc., Shizuoka, Japan).

Islet Isolation and Transplantation

Islet isolation and culture were performed as previously described (*34*). Diabetic Lewis rats underwent intraportal islet transplantation after receiving isoflurane (Abbot Japan Co., Ltd., Tokyo, Japan) for anesthesia. Rat islets were infused at a total volume of 1 mL into the recipient liver through the portal vein using a 25-gauge insulin syringe.

Induction and Diagnosis of Diabetes in the Recipients

Diabetes was induced by intravenous injection of streptozotocin (65 mg/kg) 7 days before surgery. Rats whose non-fasting blood glucose levels were ≥400 mg/dL on two consecutive measurements were considered diabetic. Serial blood glucose levels were determined, and recipients whose non-fasting blood glucose was <200 mg/dL on two consecutive measurements were considered to be cured.

Experimental Groups

Four islet equivalents (IEQs) per gram of syngeneic rat islet grafts were transplanted intraportally into three groups of streptozotocin-induced diabetic rats: the control, insulin-treated, and insulin+rest groups (868±14, 886±11, and 895±8 IEQs/rat, respectively). The control group (n=8) fed freely without insulin treatment during the study period. Both the insulin (n=5) and insulin+rest (n=7) groups received continuous insulin (Eli Lilly Japan Corp., Kobe, Japan) infusion intravenously from days 1 to 14 after transplantation by the following method. At day 1, in both groups, a small-gauge catheter was inserted into the right jugular vein under isoflurane anesthesia. The proximal end of the catheter was tunneled subcutaneously, exited between the shoulders and connected to a harness (Quick Connect Infusion System with Harness; Strategic Applications Inc., Lake Villa, IL). The catheter was then passed through a flexible and protective coil and attached via a freely rotating swivel (Strategic Applications Inc.) to an infusion pump (REGRO Digital; Ismatec SA, Glattbrugg, Switzerland).

The insulin dose was adjusted daily so that blood glucose levels were maintained between 80 and 150 mg/dL (mean dose: insulin group 1.87±0.24 U/day, resting group 1.89±0.23 U/day, P=0.91).

In addition, the insulin+rest group fasted while receiving total parenteral nutrition (TPN) from days 1 to 14 after transplantation. Nutritional support was prepared and infused under sterile conditions. The TPN solution (FULCALIQ No. 3; Tanabe Seiyaku Co., Ltd., Osaka, Japan) was composed of amino acids, dextrose, vitamins, and electrolytes. One liter contained 36.3 g of amino acids and 226.7 g of dextrose. Rats in the insulin+rest group received approximately 300 kcal/kg per day infused at 1.05 kcal/mL × 2.7 mL/h (*35–39*).

Blood Analyses

Blood samples were collected from anesthetized rats via a tail incision on days 0, 14, and 35. These samples ware centrifuged immediately for 10 min at 2,200 *g*, and the resulting serum was frozen at −80°C until the analyses. The serum levels of interleukin-6 (IL-6), monocyte chemoattractant protein-1 (MCP-1), and tumor necrosis factor-alpha (TNF-α) were determined using a MILLIPLEX MAP Kit Rat (Millipore Corp., Billerica, MA). The serum levels of 8-OHdG were determined using a Highly Sensitive ELISA kit for 8-OHdG (NIKKEN SEIL Corp., Shizuoka, Japan) to analyze the oxidative stress in the recipients. For the glucagon-like peptide-1 (GLP-1) analysis, blood samples obtained on days 0 and 14 were collected into microtubes containing a dipeptidyl peptidase 4 (DPP-4) inhibitor and centrifuged immediately for 10 min at 1,000 *g*, and then the serum was frozen at −80°C. The blood samples from the resting group on day 14 were collected under fasting conditions. The serum levels of GLP-1 were determined using a GLP-1 (Active) ELISA Kit (Shibayagi, Gunma, Japan).

Intravenous Glucose Tolerance Testing (IVGTT)

The IVGTT was performed 5 weeks after islet infusion. After a 14-hr fast, D-glucose (1.0 g/kg) was infused intravenously as a single bolus, and the blood glucose concentrations were determined before and at 5, 10, 20, 30, 60, 90, and 120 min after the glucose injection. The results of the IVGTT were evaluated by area under the curve (AUC) and Kg values.

Quantitation of Insulin in the Recipient Livers

Recipient livers were retrieved and homogenized in 5 mL of deionized water at 4°C. After adding 25 mL of deionized water and 75 mL of 0.18 M HCl in 96% ethanol, the homogenate was stored at 4°C for 24 hr and was then centrifuged at 2,150 *g* for 10 min. The resulting supernatant was stored at −80°C. The insulin concentration in the supernatant was evaluated using a commercial ELISA kit (Mercodia, Uppsala, Sweden).

Immunohistochemical Staining

The recipient livers with islet grafts were harvested and fixed with 4% paraformaldehyde overnight, and embedded in paraffin for immunohistochemical staining 14 days after transplantation. Immunohistochemical staining was performed using an In Situ Apoptosis Detection Kit (Trevigen, Inc. Gaithersburg, MD) for TUNEL staining, and an anti-von Willebrand Factor (vWF) antibody (Millipore) and Envision kit (Dako, Glostrup,

Denmark) for vWF staining. At least 35 sections from each experimental group (n=3, respectively) were evaluated for islet apoptosis by counting the TUNEL-positive cells. For the evaluation of revascularization, the number of new vessels around the grafts that consisted of vWF-positive cells was compensated by graft size. The mean number of new vessels per islet area from three individual experiments (at least 10 sections from one experiment) was compared among the three groups. The count was performed among triple-blind evaluations.

Statistical Analysis

All data are expressed as the means±SEM and were compared using a one-way factorial analysis of variance (ANOVA). The Bonferroni correction was used as a post hoc test when the data were determined to be significant by ANOVA. Differences were considered to be significant when $P<0.05$.

ACKNOWLEDGMENTS

The authors thank Kozue Imura and Megumi Goto for their excellent technical assistance, and Bo Nilsson for his assistance with editing the manuscript. The authors also acknowledge the support of the Biomedical Research Core of Tohoku University, Graduate School of Medicine and TAMRIC (Tohoku Advanced Medical Research and Incubation Center).

REFERENCES

1. Menger MD, Vajkoczy P, Leiderer R, et al. Influence of experimental hyperglycemia on microvascular blood perfusion of pancreatic islet isografts. *J Clin Invest* 1992; 90: 1361.
2. Menger MD, Jaeger S, Walter P, et al. Angiogenesis and hemodynamics of microvasculature of transplanted islets of Langerhans. *Diabetes* 1989; 38(Suppl 1): 199.
3. Andersson A, Korsgren O, Jansson L. Intraportally transplanted pancreatic islets revascularized from hepatic arterial system. *Diabetes* 1989; 38(Suppl 1): 192.
4. Ar'Rajab A, Ahren B. Prevention of hyperglycemia improves the long-term result of islet transplantation in streptozotocin-diabetic rats. *Pancreas* 1992; 7: 435.
5. Merino JF, Nacher V, Raurell M, et al. Optimal insulin treatment in syngeneic islet transplantation. *Cell Transplant* 2000; 9: 11.
6. Pakhomov O, Honiger J, Gouin E, et al. Insulin treatment of mice recipients preserves beta-cell function in porcine islet transplantation. *Cell Transplant* 2002; 11: 721.
7. Juang JH, Bonner-Weir S, Wu YJ, et al. Beneficial influence of glycemic control upon the growth and function of transplanted islets. *Diabetes* 1994; 43: 1334.
8. Ferrer-Garcia JC, Merino-Torres JF, Perez Bermejo G, et al. Insulin-induced normoglycemia reduces islet number needed to achieve normoglycemia after allogeneic islet transplantation in diabetic mice. *Cell Transplant* 2003; 12: 849.
9. Merino JF, Nacher V, Raurell M, et al. Improved outcome of islet transplantation in insulin-treated diabetic mice: effects on beta-cell mass and function. *Diabetologia* 1997; 40: 1004.
10. Koh A, Senior P, Salam A, et al. Insulin-heparin infusions peritransplant substantially improve single-donor clinical islet transplant success. *Transplantation* 2010; 89: 465.
11. Dafoe DC, Campbell DA Jr, Rosenberg L, et al. No improvement of pancreas transplant endocrine function by exogenous insulin infusion (islet rest) in the postoperative period. *Transplantation* 1989; 48: 22.
12. Keymeulen B, Vetri M, Gorus F, et al. The effect of insulin treatment on function of intraportally grafted islets in streptozotocin-diabetic rats. *Transplantation* 1993; 56: 60.
13. Leahy JL, Bonner-Weir S, Weir GC. Beta-cell dysfunction induced by chronic hyperglycemia. Current ideas on mechanism of impaired glucose-induced insulin secretion. *Diabetes Care* 1992; 15: 442.
14. Biarnes M, Montolio M, Nacher V, et al. Beta-cell death and mass in syngeneically transplanted islets exposed to short- and long-term hyperglycemia. *Diabetes* 2002; 51: 66.
15. Korsgren O, Jansson L, Andersson A. Effects of hyperglycemia on function of isolated mouse pancreatic islets transplanted under kidney capsule. *Diabetes* 1989; 38: 510.
16. Eizirik DL, Jansson L, Flodstrom M, et al. Mechanisms of defective glucose-induced insulin release in human pancreatic islets transplanted to diabetic nude mice. *J Clin Endocrinol Metab* 1997; 82: 2660.
17. Gerrits AJ, Koekman CA, Yildirim C, et al. Insulin inhibits tissue factor expression in monocytes. *J Thromb Haemost* 2009; 7: 198.
18. Aljada A, Ghanim H, Mohanty P, et al. Insulin inhibits the pro-inflammatory transcription factor early growth response gene-1 (Egr)-1 expression in mononuclear cells (MNC) and reduces plasma tissue factor (TF) and plasminogen activator inhibitor-1 (PAI-1) concentrations. *J Clin Endocrinol Metab* 2002; 87: 1419.
19. White MF. Insulin signaling in health and disease. *Science* 2003; 302: 1710.
20. Johnson JD, Bernal-Mizrachi E, Alejandro EU, et al. Insulin protects islets from apoptosis via Pdx1 and specific changes in the human islet proteome. *Proc Natl Acad Sci U S A* 2006; 103: 19575.
21. Yanjun W, Yue X, Shixing L. Effect of blood glucose fluctuation on the function of rat pancreatic islets in vivo. *Regul Pept* 2011.
22. Sato Y, Endo H, Okuyama H, et al. Cellular hypoxia of pancreatic {beta}-cells due to high levels of oxygen consumption for insulin secretion in vitro. *J Biol Chem* 2011; 286: 12524.
23. Yamada Y, Fukuda K, Fujimoto S, et al. SUIT, secretory units of islets in transplantation: an index for therapeutic management of islet transplanted patients and its application to type 2 diabetes. *Diabetes Res Clin Pract* 2006; 74: 222.
24. Hoogma RP, Hammond PJ, Gomis R, et al. Comparison of the effects of continuous subcutaneous insulin infusion (CSII) and NPH-based multiple daily insulin injections (MDI) on glycaemic control and quality of life: results of the 5-nations trial. *Diabet Med* 2006; 23: 141.
25. Catargi B, Breilh D, Gin H, et al. A randomized study comparing blood glucose control and risk of severe hypoglycemia achieved by non-programmable versus programmable external insulin pumps. *Diabetes Metab* 2001; 27: 323.
26. Veriter S, Aouassar N, Adnet PY, et al. The impact of hyperglycemia and the presence of encapsulated islets on oxygenation within a bioartificial pancreas in the presence of mesenchymal stem cells in a diabetic Wistar rat model. *Biomaterials* 2011; 32: 5945.
27. Leibiger IB, Leibiger B, Berggren PO. Insulin signaling in the pancreatic beta-cell. *Annu Rev Nutr* 2008; 28: 233.
28. Okada T, Liew CW, Hu J, et al. Insulin receptors in beta-cells are critical for islet compensatory growth response to insulin resistance. *Proc Natl Acad Sci U S A* 2007; 104: 8977.
29. Persaud SJ, Muller D, Jones PM. Insulin signalling in islets. *Biochem Soc Trans* 2008; 36(Pt 3): 290.
30. Wang Q, Jin T. The role of insulin signaling in the development of beta-cell dysfunction and diabetes. *Islets* 2009; 1: 95.
31. Farilla L, Hui H, Bertolotto C, et al. Glucagon-like peptide-1 promotes islet cell growth and inhibits apoptosis in Zucker diabetic rats. *Endocrinology* 2002; 143: 4397.
32. Bregenholt S, Moldrup A, Blume N, et al. The long-acting glucagon-like peptide-1 analogue, liraglutide, inhibits beta-cell apoptosis in vitro. *Biochem Biophys Res Commun* 2005; 330: 577.
33. Bayne K. Revised Guide for the Care and Use of Laboratory Animals available. American Physiological Society. *Physiologist* 1996; 39: 199, 208–11.
34. Saito Y, Goto M, Maya K, et al. Brain death in combination with warm ischemic stress during isolation procedures induces the expression of crucial inflammatory mediators in the isolated islets. *Cell Transplant* 2010; 19: 775.
35. Raftogianis RB, Franklin MR, Galinsky RE. Effect of lipid-free total parenteral nutrition on hepatic drug conjugation in rats. *J Pharmacol Exp Ther* 1996; 276: 602.
36. Bojanowska E, Radziszewska E. Combined stimulation of glucagon-like peptide-1 receptor and inhibition of cannabinoid CB1 receptor act synergistically to reduce food intake and body weight in the rat. *J Physiol Pharmacol* 2011; 62: 395.
37. Hagiwara S, Iwasaka H, Shingu C, et al. Effect of enteral versus parenteral nutrition on inflammation and cardiac function in a rat model of endotoxin-induced sepsis. *Shock* 2008; 30: 280.
38. Hagiwara S, Iwasaka H, Kusaka J, et al. Total parenteral-nutrition-mediated dendritic-cell activation and infiltration into the small intestine in a rat model. *J Anesth* 2011; 25: 57.
39. Montano ME, Molpeceres V, Mauriz JL, et al. Effect of melatonin supplementation on food and water intake in streptozotocin-diabetic and non-diabetic male Wistar rats. *Nutr Hosp* 2010; 25: 931.

ELSEVIER

Edaravone, a Free Radical Scavenger, Improves the Graft Viability on Liver Transplantation From Non–heart-beating Donors in Pigs

K. Miyazawa[a,*], S. Miyagi[a], K. Maida[a], K. Murakami[a], A. Fujio[a], T. Kashiwadate[a], W. Nakanishi[a], Y. Hara[a], C. Nakanishi[a], H. Yamaya[a], N. Kawagishi[a], M. Goto[b], and N. Ohuchi[a]

[a]Division of Advanced Surgical Science and Technology, Graduate School of Medicine, Tohoku University, Sendai, Miyagi, Japan; and [b]Division of Advanced Cell Transplantation, Graduate School of Medicine, Tohoku University, Sendai, Miyagi, Japan

ABSTRACT

Background. Although liver transplantation from non–heart-beating donors (NHBDs) is an effective way to overcome shortage of donors, primary graft nonfunction is often noted in these grafts. We have previously reported that edaravone, a free radical scavenger, has a cytoprotective effect on warm ischemia-reperfusion injury and improves the function of liver grafts from NHBDs in a rat model of ischemia-reperfusion. The purpose of this study was to investigate the effects of edaravone on liver transplantations from NHBDs.

Methods. Pigs were divided into three groups: (1) a heart-beating (HB) group (n = 5), in which liver grafts were retrieved from HB donors; (2) a non-heart-beating (NHB) group (n = 4), in which liver grafts were retrieved under apnea-induced NHB conditions; and (3) an edaravone-treated (ED) group (n = 5), in which liver grafts were retrieved in the same manner as the NHB group and treated with edaravone at the time of perfusion (3 mg/L in University of Wisconsin [UW] solution), cold preservation (1 mg/L in UW solution), and after surgery (1 mg/kg/d). The grafts from all groups were transplanted after 4 hours of cold preservation.

Results. In the ED group, the 7-day survival rate was significantly higher than that in the NHB group (80% versus 0%, $P = .0042$, Kaplan-Meier log-rank test). Furthermore, on histologic examination, the structure of sinusoids in the ED group was well preserved and similar to that in the HB group.

Conclusions. Edaravone may improve the viability of liver grafts from NHBDs.

LIVER transplantation (LT) is an established treatment for end-stage liver diseases. However, worldwide, this treatment is limited by a shortage of donors. LT from non–heart-beating donors (NHBDs) is an effective way to overcome this problem. However, primary graft nonfunction along with biliary complications is often reported in liver grafts from NHBDs [1]. In the early stage of ischemia-reperfusion, one critical component in causing hepatocellular injury is reactive oxygen species (ROS), which can directly inflict cellular damage and mediate inflammatory cascades.

We have previously reported that edaravone, a free radical scavenger, has a cytoprotective effects on warm ischemia-reperfusion injury and improves the function of liver grafts from NHBDs in a rat model of the ischemia-reperfusion (Fig 1) [2,3]. The purpose of this study was to investigate the effects of edaravone on LT from NHBDs.

METHODS

All experiments were conducted according to the *Guide for the Care and Use of Laboratory Animals* prepared by National Academy of Sciences and published by the National Institutes of Health.

Experimental Design

Male pigs, F1 hybrid of Landrace × Large White, weighing 25 to 29 kg, were divided into three groups: (1) a heart-beating (HB) group (n = 5), in which liver grafts were retrieved from HB donors; (2) a non–heart-beating (NHB) group (n = 4), in which liver grafts were retrieved under apnea-induced NHB conditions; (3) an

*Address correspondence to Koji Miyazawa, The Division of Advanced Surgical Science and Technology, Graduate School of Medicine, Tohoku University, 1-1 Seiryo-machi, Aoba-ku, Sendai 980-8574, Japan. E-mail: miyazawa_koji@yahoo.co.jp

0041-1345/14/$–see front matter
http://dx.doi.org/10.1016/j.transproceed.2013.11.155

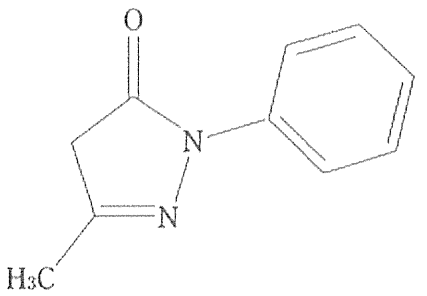

Fig 1. Chemical structure of edaravone (3-methyl-1-phenyl-2-pyrazolin-5-one).

edaravone-treated (ED) group (n = 5), in which liver grafts were retrieved in the same manner as the NHB group and treated with edaravone at the time perfusion (3 mg/L in University of Wisconsin [UW] solution), cold preservation (1 mg/L in UW solution), and after surgery (1 mg/kg/d).

The grafts from all groups were transplanted after 4 hours cold preservation.

Donor Operation

The pigs were premedicated with intramuscular meloxicam, anesthetized with intramuscular medetomidine (0.1 mL/kg) and midazolam (0.1 mL/kg), and maintained with an isoflurane/oxygen mixture, pancuronium bromide, and buprenorphine hydrochloride. A catheter was placed in the external jugular vein for blood sampling and intravenous infusion, and another was placed in the common carotid artery for monitoring the blood pressure. The process of liver retrieval was similar to that followed in human donors, with minor modifications. First, the common bile duct was cannulated. After intravenous heparin (300 U/kg) was administered, the splenic vein and abdominal aorta were cannulated. In the NHB group and the ED group, the donor's respiration was stopped by using pancuronium bromide and detaching the respirator. Ten minutes after cardiac arrest, the liver graft was perfused with cold Ringer's lactate solution and subsequently with 1000 mL UW solution (DuPont Pharmaceuticals, Wilmington, Del, United States) through the portal vein and abdominal aorta. The liver graft was retrieved immediately after flushing and preserved in cold UW solution for 4 hours at 4°C. In the ED group, the liver graft was treated with edaravone at the time of the perfusion (3 mg/L in UW solution) and was cold preserved (1 mg/L in UW solution). In the HB group, the liver graft was procured as mentioned above, but not in the agonal state.

Recipient Operation

The recipient pigs were anesthetized in the same way as the donors. A catheter was placed in the external jugular vein for blood sampling and intravenous infusion, and another was placed in the common carotid artery for monitoring of the blood pressure. After intravenous heparin (300 U/kg) administration, the liver was dissected and removed. During the anhepatic phase, the portal vein blood was shunted to the left jugular vein, and the infrahepatic inferior vena cava to the right jugular vein using an Anthron bypass tube (Toray, Tokyo, Japan). The liver graft was implanted orthotopically with end-to-end anastomosis of the suprahepatic inferior vena cava (with 4-0 Prolene, running suture), the portal vein (with 6-0 Prolene, running suture), the infrahepatic inferior vena cava (with 4-0 Prolene, running suture), and the hepatic artery (with 9-0 nylon, intermittent suture, microsurgically). The liver graft was reperfused with portal blood after completion of the portal vein anastomosis. The bile duct was drained through an external tube fistula. In the ED group, intravenous edaravone (1 mg/kg/d) was administered during the first 3 postoperative days. The recipients were sacrificed on postoperative day 7.

Aspartate aminotransferase (AST), lactate dehydrogenase (LDH) and tumor necrosis factor-α (TNF-α) level were measured using commercially available kits: AST (Iatron Laboratories, Osaka, Japan); LDH (Wako Pure Chemical Industries, Osaka, Japan); TNF-α (R&D Systems, Minneapolis, MN, United States).

Histologic Examination

The specimens were stained with hematoxylin and eosin for light microscopic examination.

Statistical Analysis

All the calculations were made with the JMP Pro software package (SAS Institute, Cary, NC, United States). The results were expressed as mean values ± standard deviations. A statistical analysis was performed using one-factor analysis of variance and Tukey's honestly significant different test. Kaplan-Meier survival curves were constructed for both study groups. The effects of management on overall survival were examined initially using the Kaplan-Meier log-rank test.

RESULTS

Recipient Survival

In the HB group, all five recipients survived for >7 days, whereas three recipients in the NHB group died within 24 hours after the transplantation. In the ED group, four recipients survived for >7 days, which was a significantly higher survival rate than that of the NHB group (80% versus 0%, $P = .0042$, Kaplan-Meier log-rank test, Table 1, Fig 2).

Serum AST and LDH

Serum AST and LDH increased after reperfusion in all groups and remained high on postoperative day 1, but they subsequently decreased with time. There were no statistical differences between the ED and the NHB groups in any phase (Fig 3).

Table 1. Recipient Survival After Liver Transplantation

Group	Survival	Cause of Death
HB (n = 5)	>7 days	Sacrificed
	>7 days	Sacrificed
	>7 days	Sacrificed
	>7 days	Sacrificed
	>7 days	Sacrificed
NHB (n = 4)	4 days	Primary graft failure
	<24 hours	Primary graft failure
	<24 hours	Primary graft failure
	<24 hours	Primary graft failure
ED (n = 5)	>7 days	Sacrificed
	>7 days	Sacrificed
	>7 days	Sacrificed
	>7 days	Sacrificed
	<24 hours	Primary graft failure

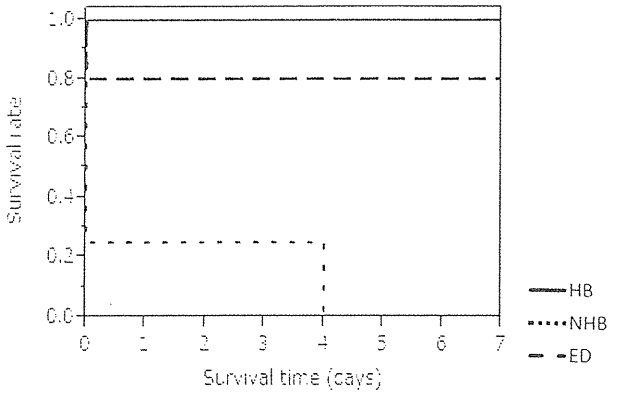

Fig 2. Survival curve of the recipient after liver transplantation.

Serum TNF-α

Serum TNF-α increased after reperfusion in all groups, and it subsequently decreased with time. There were no statistical differences between the ED and the NHB groups during any phase (Fig 4).

Histologic Examination

Histologic examination revealed that 1 hour after reperfusion, the sinusoidal spaces in the NHB group were narrow compared with those in the other groups. In the NHB group, deterioration of sinusoidal endothelial cells, hepatocellular swelling, and vacuolation were more severe than those in the other groups (Fig 5).

DISCUSSION

LT has become the standard therapy for end-stage liver disease. However, a shortage of donors has become a serious problem. Some institutes attempted to use grafts retrieved from NHBDs, but the results of these transplantations have been poor, particularly in cases of uncontrolled NHBD [4,5]. It is well known that the presence of warm ischemia before retrieval of the liver graft induces severe damage to the graft after cold preservation [6].

We have reported that the generation of free radical, Kupffer cell activation, release of TNF-α, and activation of

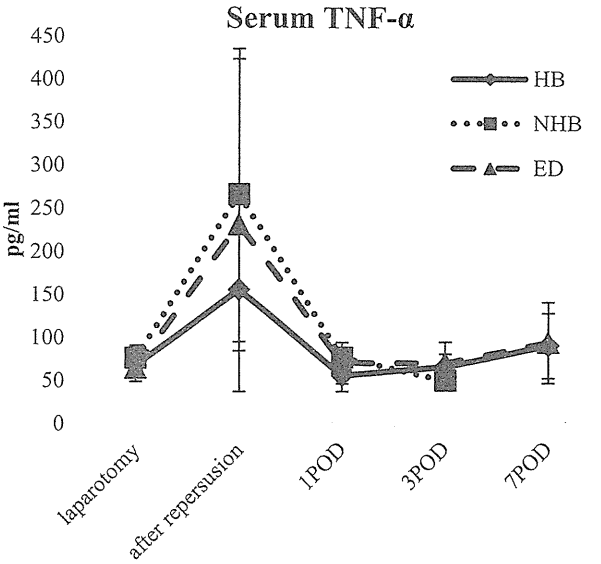

Fig 4. Serum TNF-α levels (HB, heart-beating group; NHB, non-heart-beating group; ED, edaravone treated group. Data are given as mean [SD]).

neutrophils play important roles in the development of reperfusion injury [7–9]. Recent studies have shown that the preservation of the microcirculation as well as reduction of free radicals and inflammatory cytokines play important roles in improving the energy status and viability of liver grafts from NHBD [10].

In the pathogenesis of ischemia-reperfusion injury, ROS appeared to be implicated in various ways. ROS derived from activated endothelial cells and Kupffer cells during ischemia-reperfusion cause direct oxidative damage to DNA, proteins, and lipids, leading to cell death. Several investigators reported cytoprotective effects of edaravone on warm ischemia-reperfusion injury using cold or reperfusion injury models [2,3,11,12].

In this study, we examined the protective effects of edaravone on the structure and function of liver grafts from warm ischemia-reperfusion injury in actual liver transplantations from NHBDs. The results revealed that edaravone preserved the sinusoidal structure and improved the

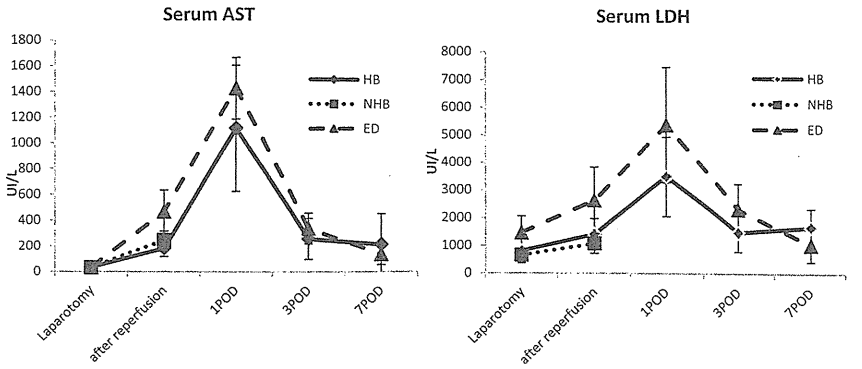

Fig 3. Serum AST and LDH levels (HB, heart-beating group; NHB, non-heart-beating group; ED, edaravone treated group. Data are given as mean SD).

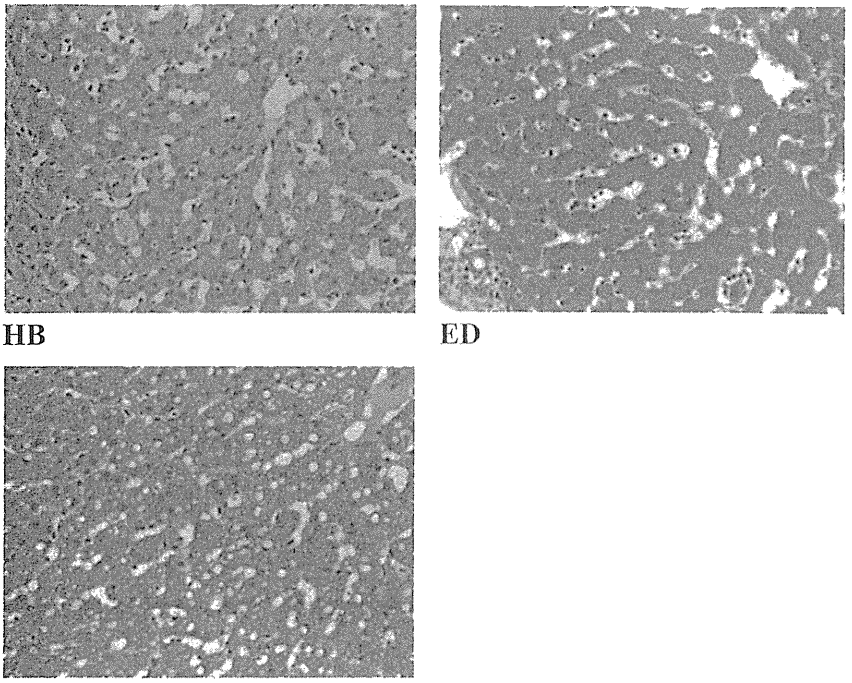

Fig 5. Microphotographs of the liver grafts 1 hour after reperfusion (hematoxylin and eosin stain, original magnification × 400; HB, heart-beating group; NHB, non-heart-beating group; ED, edaravone-treated group).

viability of liver grafts from NHBDs. This is the first study to analyze the effect of edaravone on the agonal warm ischemia reperfusion in a LT model of large animals such as pigs.

In several studies, animals were treated with edaravone (1 to 8.71 mg/L) in perfusion solution. For the treatment of acute cerebral infarction in a clinical situation, edaravone is administered at 1 mg/kg/d and the concentration of edaravone in blood is estimated to be approximately 1 mg/L. It appears that it is important to administer sufficient amount of edaravone at an early phase of warm ischemia reperfusion injury. Thus, we used edaravone at 3 mg/L in perfusion solution. We used edaravone at 1 mg/L in preservation solution and at 1 mg/kg/d (intravenously) postoperatively in the clinical situation.

In this study, the apnea-induced agonal NHB model was selected because it is the model closest to the uncontrolled NHBD. The livers from uncontrolled NHBDs were negatively affected not only by warm ischemia but also by intestinal ischemia. In contrast, the usual NHBD model induced by potassium chloride injection or aortic clamping appeared to lack the influences of the hypoxic or ischemic intestine because portal blood flow stops immediately after the induction of warm ischemia. We believe that our NHBD model is suitable for the investigation of marginal donors, including NHBDs.

Sinusoid narrowing reflects hepatocyte swelling and the disruption of sinusoidal endothelial cells; furthermore, the narrowing leads to disturbance in microcirculation and deterioration of graft function [7,10]. Several studies have indicated that the death of sinusoidal endothelial cells after microcirculatory disturbance and imbalance of vasoconstrictors were induced by ROS. In our study, the sinusoidal space was well preserved in the ED group compared with that in the NHB group. Furthermore, deterioration of sinusoidal endothelial cells, hepatocellular swelling, and vacuolation were suppressed in the ED group.

We observed a significant difference in the survival rate between the ED and NHB groups. These results suggest that edaravone may be effective in improving the viability of marginal donor grafts, including NHBD.

In conclusion, edaravone could protect the structure and function of liver grafts from warm ischemia-reperfusion injury and improve the viability of liver grafts from NHBDs. Although further investigation is necessary, the treatment of liver grafts from NHBDs with edaravone appears to be a promising strategy to improve graft viability in LT from NHBDs.

REFERENCES

[1] Otero A, Gómez-Gutiérrez M, Suárez F, et al. Liver transplantation from Maastricht category 2 non-heart-beating donors. Transplantation 2003;76:1068–73.

[2] Nakamura A, Akamatsu Y, Miyagi S, et al. A free radical scavenger, edaravone, prevents ischemia-reperfusion injury in liver grafts from non-heart-beating donors. Transplant Proc 2008;40: 2171–4.

[3] Kobayashi Y, Akamatsu Y, Iwane T, et al. Signaling pathway on the effect of oxygenated warm perfusion prior to cold preservation of the liver grafts from non-heart-beating donors, and the additive effect of edaravone. Transplant Proc 2009;41:49–51.

[4] Reddy S, Zlivetti M, Brockmann J, et al. Liver transplantation from non-heart-beating donors: current status and future prospects. Liver Transpl 2004;10:1223–32.

[5] Totsuka E, Fung JJ, Hakamada K, et al. Experience of orthotopic liver transplantation from non-heart-beating donors at the University of Pittsburgh Medical Center. Nippon Geka Gakkai Zasshi 1999;100:818–21.

[6] Lutterová M, Szatmáry Z, Kukan M, et al. Marked difference in tumor necrosis factor-alpha expression in warm ischemia- and cold ischemia-reperfusion of the rat liver. Cryobiology 2000;41:301–14.

[7] Miyagi S, Ohkohchi N, Okikawa K, et al. Effects of anti-inflammatory cytokine agent (FR167653) and serine protease inhibitor on warm ischemia-reperfusion injury of the liver graft. Transplantation 2004;77:1487–93.

[8] Shibuya H, Ohkohchi N, Seya K, et al. Kupffer cells generate superoxide anions and modulate reperfusion injury in rat livers after cold preservation. Hepatology 1997;25:356–60.

[9] Shibuya H, Ohkohchi N, Tsukamoto S, et al. Tumor necrosis factor-induced, superoxide-mediated neutrophil accumulation in cold ischemic/reperfused rat liver. Hepatology 1997;26: 113–20.

[10] Tsukamoto S, Ohkohchi N, Fukumori T, et al. Elimination of Kupffer cells and nafamostat mesilate rinse prevent reperfusion injury in liver grafts from agonal non-heart-beating donors. Transplantation 1999;67:1396–403.

[11] Ninomiya M, Shimada M, Harada N, et al. The hydroxyl radical scavenger MCI-186 protects the liver from experimental cold ischaemia-reperfusion injury. Br J Surg 2004;91:184–90.

[12] Shimoda M, Iwasaki Y, Okada T, et al. Edaravone inhibits apoptosis caused by ischemia/reperfusion injury in a porcine hepatectomy model. World J Gastroenterol 2012;21:3520–6.

Glycobiology vol. 24 no. 2 pp. 125–138, 2014
doi:10.1093/glycob/cwt088
Advance Access publication on October 7, 2013

A comparison of the main structures of *N*-glycans of porcine islets with those from humans

Shuji Miyagawa[1,2], Akira Maeda[2], Takuji Kawamura[2], Takehisa Ueno[2], Noriaki Usui[2], Sachiko Kondo[3], Shinichi Matsumoto[4], Teru Okitsu[5], Masafumi Goto[6], and Hiroshi Nagashima[7]

[2]Division of Organ Transplantation, Department of Surgery, Osaka University Graduate School of Medicine, Osaka, Japan; [3]GLYENCE Co., Ltd., Aichi, Japan; [4]National Center for Global Health and Medicine, Tokyo, Japan; [5]Institute of Industrial Science, University of Tokyo, Tokyo, Japan; [6]Tohoku University International Advanced Research and Education Organization, Tohoku University, Miyagi, Japan; and [7]Laboratory of Developmental Engineering, Department of Life Science, Meiji University, Kanagawa, Japan

Received on December 18, 2012; revised on September 27, 2013; accepted on September 30, 2013

After producing α1-3-galactosyltransferase knockout (GKO) pigs, most of the organs of these pigs showed less antigenicity to the human body. However, wild-type adult pig islets (API) that originally contained negligible levels of α-galactosidase now showed a clear antigenicity to human serum. In this study, *N*-glycans were isolated from both APIs and human islets. Their structures were then analyzed by a mapping technique based on their high-performance liquid chromatography elution positions and matrix-assisted laser desorption/ionization-time-of-flight mass spectrometric data. Both preparations contained substantial amounts of high-mannose structures. The *N*-glycans from human islets were separated into 17 neutral, 8 mono-sialyl and 4 di-sialyl glycans, and the API glycans were comprised of 11 neutral, 8 mono-sialyl, 3 di-sialyl, 2 mono-sulfated, 3 mono-sialyl-mono-sulfated and 1 di-sulfated glycans. Among them, the API preparation contained one neutral, five mono-sialyl glycans and six sulfated glycans that were not detected in human islets. The structures of 9 of these 12 could be clearly determined. In addition, a study of the sulfate-depleted API suggests that sulfate residues could be antigenic to humans. The data herein will be helpful for future studies of the antigenicity associated with API.

Keywords: *N*-glycan / pig islets / sulfated glycan / xenotransplantation

Introduction

The increasing challenges associated with the worldwide shortage of donor organs have led to a renewed interest in xenotransplantation. The pig pancreas is considered to be the most suitable source of islets for clinical xenotransplantation. Some clinical trials have resumed in New Zealand, Russia, etc., using islets from a wild-type pig via the use of an immuno-isolation technique (Elliott 2011). In addition, based on data collected from the "Inventory of human xenotransplantation practices" (http://www.humanxenotransplant.org/index.html), many clinical trials appear to be ongoing.

On the other hand, after producing α1-3-galactosyltransferase knockout (GKO) pigs (Dai et al. 2002; Takahagi et al. 2005), most of the organs from these pigs were found to show less antigenicity to the human body. However, wild-type adult pig islets (API) that originally contained negligible levels of α-galactosidase (α-Gal) (Galα1-3Gal) (Galili et al. 1987) showed a clear antigenicity to human serum (Komoda et al. 2004), and this fact represents a significant obstacle to successful xenotransplantation (Thompson et al. 2011).

Concerning the so-called non-Gal epitopes, many studies related to glycoproteins and glycolopids are on-going in attempts to identify them. However, our knowledge of non-Gal glycoantigens is still incomplete. That is, previous analyses of *N*-glycans from pigs included the use of additional tissues, in addition to islets. However, besides α-Gal and Hanganutziu-Deicher (Varki et al. 2009; Yamamoto et al. 2013) antigen expression, the glycosylation of API remains relatively unclear (Breimer 2011; Byrne et al. 2011; Miyagawa et al. 2012).

We wish to report herein on the analysis of the glycosylation of the *N*-linked sugars of API, compared with the corresponding values for human islets, using a high-performance liquid chromatography (HPLC) technique, which is capable of providing reliable data. The collected data will be of use in future research concerning non-Gal antigens and promises to provide us with clues for producing new types of immuno-modified pigs with less antigenicity than GKO pigs.

Results

Isolation of N-*glycans of the porcine and human islets*

N-glycans derived from porcine (11.9 mg of protein) and human islets (12.47 mg of protein) were separated into five peaks, based on increasing acidity using a diethylaminoethyl (DEAE) column. The following peaks were produced: Neutral

[1]To whom correspondence should be addressed: e-mail: miyagawa@orgtrp.med.osaka-u.ac.jp

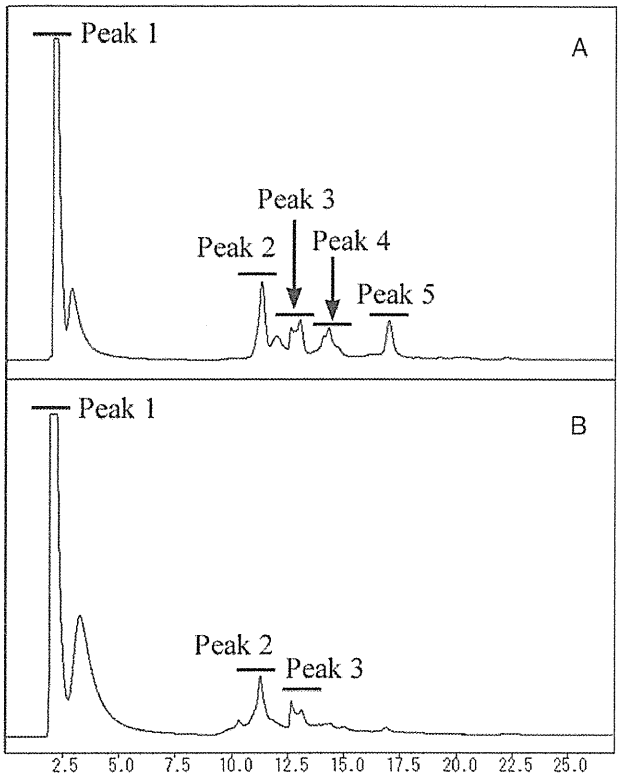

Fig. 1. Anion exchange DEAE elution profiles of PA-glycans derived from porcine islets (**A**) and the human islets (**B**). The PA-glycans were fractionated according to their sialic acid content and sulfate residues as neutral (Peak 1), mono-sialyl (Peak 2), di-sialyl or mono-sulfate (Peak 3), mono-sialyl-mono-sulfate (Peak 4) and di-sulfate (Peak 5) oligosaccharide fractions as indicated.

(N), Peak 1; mono-sialyl (M), Peak 2; di-sialyl (D) or mono-sulfate (S1), Peak 3; mono-sialyl-mono-sulfate (MS2), Peak 4 and di-sulfate (S2), Peak 5; glycan fractions with molar ratios (peak areas) of 84.4, 3.6, 2.6, 2.2 and 7.2% from APIs, and 94.0, 4.0, 2.0, 0 and 0% from the human islets, respectively (Figure 1).

Concerning API, when an octa decyl silyl (ODS) column was used, it was possible to separate the neutral fraction into fractions N1–N9, the mono-sialyl fraction into fractions M1–M6, the di-sialyl or mono-sulfate fraction into fractions D1–D3 and S1, the mono-sialyl-mono-sulfate fraction into fractions MS1–MS3 and the di-sulfate fraction into fraction S2. On the other hand, in the case of human islets, the neutral fraction was separated into N1–N13, the mono-sialyl into M1–M6 and the di-sialyl into D1–D4, as shown in Figure 2A–H.

Further analysis with GALAXY database

These ODS fractions were individually fractionated on an amide column and further subjected to matrix-assisted laser desorption/ionization time-of-flight mass spectrometric (MALDI-TOF-MS) analysis. The porcine N2, N6, M2, M3 and S1 and the human N2, N5, N6, N12, M2 and M4 fractions were found to contain two kinds of *N*-glycans (Figures 3 and 4).

The coordinates of all of the *N*-glycans coincided with those for known references in the glycoanalysis by the three axes of MS and chromatography (GALAXY) database except for several *N*-glycan fractions including human fractions N5-1, N5-2, N6-1, N6-2, M1, M2-2 and porcine S1-1, MS1and MS3. Most of the *N*-glycan structures were then identified by the mapping technique on the basis of their HPLC elution positions and MALDI-TOF-MS data.

Structural analysis of each sample

Pyridylamino (PA)-glycans, which did not correspond to any of the *N*-glycans so far registered in GALAXY, were trimmed by treatment with an exoglycosidase, which produced known glycans (Yagi et al. 2005).

In the case of S1-2, no reactivity was detected by β-acethyl-hexiominidase. Next, a methanolysis treatment induced the conversion of S1-2 into S1-2a, but additional treatment with β-galactosidase resulted in no change to S1-2a. Moreover, the β-*N*-acethylhexosaminidase treatment converted S1-2a into S1-2b, and S1-2b was proved to be the same structure as M4.1 in GALAXY, as evidenced by the observation that samples of S1-2b and M4.1 co-chromatographed (Figure 5).

The MS2 sample was analyzed following a similar procedure. The sample did not serve as a substrate for β-galactosidase and α2,3-sialydase, but was converted into MS2a by treatment with α-sialydase. Further methanolysis and β-galactosidase converted MS2a into MS2b and MS2c, respectively. MS2b was next verified to be 210.4a in GALAXY by the co-chromatography of both samples. On the other hand, MS2c, when treated with β-*N*-acethylhexosaminidase and methanolysis, was converted into MS2d and MS2e, respectively. MS2e was also proved to be 110.4a in GALAXY by the co-chromatography of both samples (Figure 6).

Concerning S2, the sample was unchanged as a result of a β-*N*-acethylhexosaminidase treatment. On the other hand, a methanolysis treatment cleaved two sulfate residues from S2 and produced S2a, which was shown to be 210.4b in GALAXY by the co-chromatography of both samples (Figure 7).

In the analyses, a total of 28 and 29 *N*-glycan structures of API and human islets, respectively, were identified and the findings are summarized in Tables I–VI (Supplementary data, Figure S1).

Sodium chlorate treatment on pig islets

The effect of removal of the sulfate structures of pig islets on the antigenicity to human serum was investigated. The use of a sodium chlorate and a sulfate-free medium led to a significant reduction in antigenicity to human serum, suggesting that the sulfate structures in adult islets are targets for human natural antibodies (Figure 8).

Discussion

Twenty-eight kinds of *N*-linked glycans were identified in the case of the API glycans and 29 were identified from human islets, based on their HPLC elution peaks. While the human preparation contained neutral, mono-sialyl, di-sialyl *N*-linked glycans, the API sample contained not only these three types, but mono-sulfate, MS2 and di-sulfate types of *N*-linked glycans

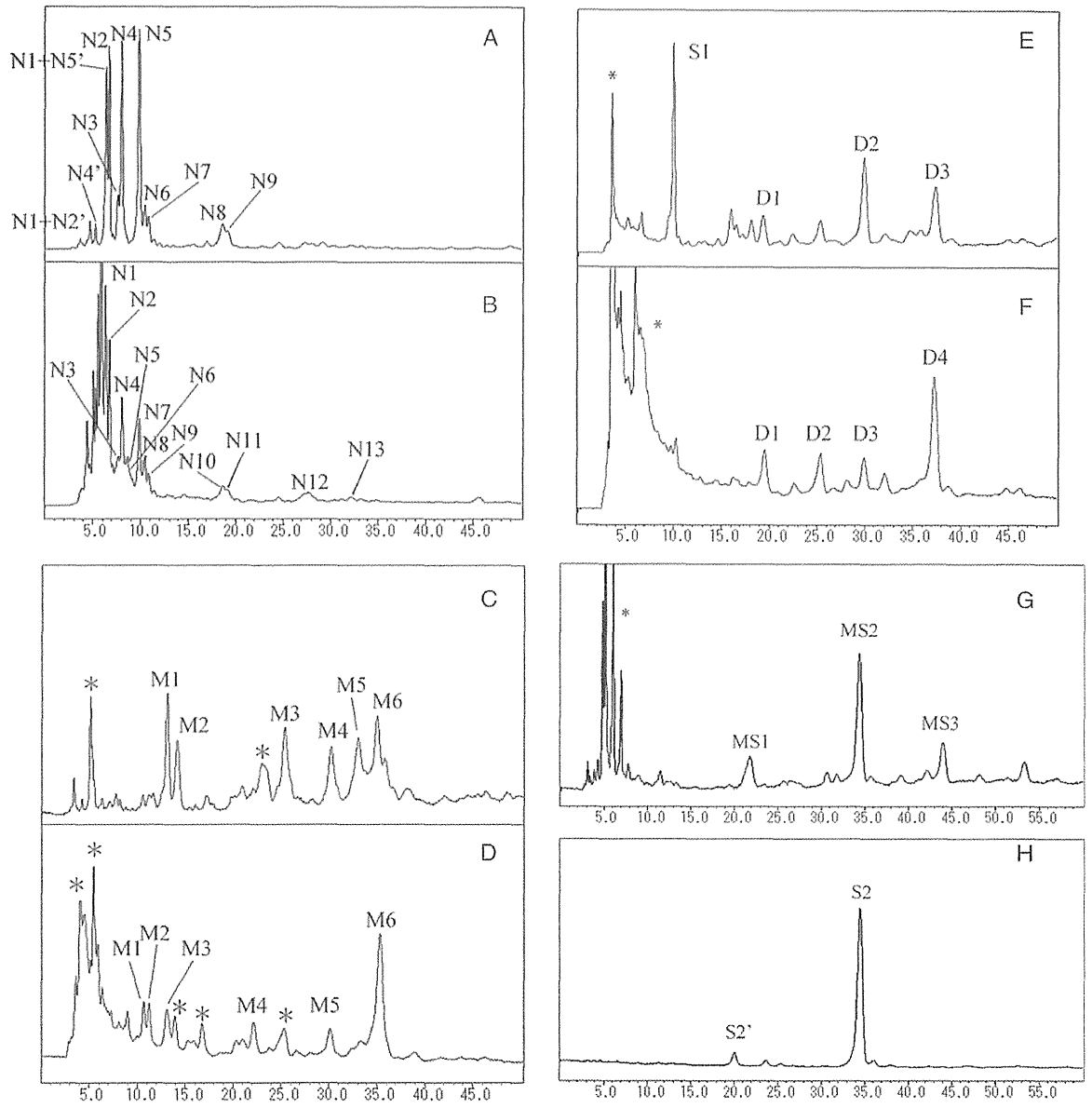

Fig. 2. Reverse-phase ODS elution profiles of PA-glycans obtained from each different fraction separated on the DEAE column. The neutral, mono-sialyl, di-sialyl or mono-sulfate, mono-sialyl-mono-sulfate and di-sulfate fractions were individually applied to the ODS column and gave elution profiles according to their hydrophobicity. (**A**) pig Peak 1, (**B**) human Peak 1, (**C**) pig Peak 2, (**D**) human Peak 2, (**E**) pig Peak 3, (**F**) human Peak 3, (**G**) pig Peak 4 and (**H**) pig Peak 5. N2′: Epimerization of N2; N4′: Epimerization of N4; N5′: Epimerization of N5; S2′: Epimerization of S2. Asterisks indicate the fractions containing no detectable PA-oligosaccharides.

as well. Among them, one neutral, five mono-sialyl and six sulfates of *N*-linked glycans in the API preparation were not detected in human islets. The structures of 9 of these 12 glycans were clearly identified in this study.

Concerning the characteristics of the *N*-glycans identified in the API preparation, the neutral glycans contained relatively high levels (%) of high-mannose type glycans. In comparison with the *N*-glycans from human islets, the high-mannose type of *N*-glycan found in API contains high levels (5 or 6) of mannoses. In addition, glycans with structures of fractions N6-2 were not detected in human islets. On the other hand, in the case of API, the relative content of sulfated *N*-glycans approached 10%. In addition, the di-sulfate type glycans represented 7% of the relative quantity, indicating that sulfated *N*-glycans are a common structure in *N*-glycans of API but do not appear to be produced by human islets. In addition, all the sulfates are attached to a β-linked *N*-acetylgalactosamine (GalNAc).

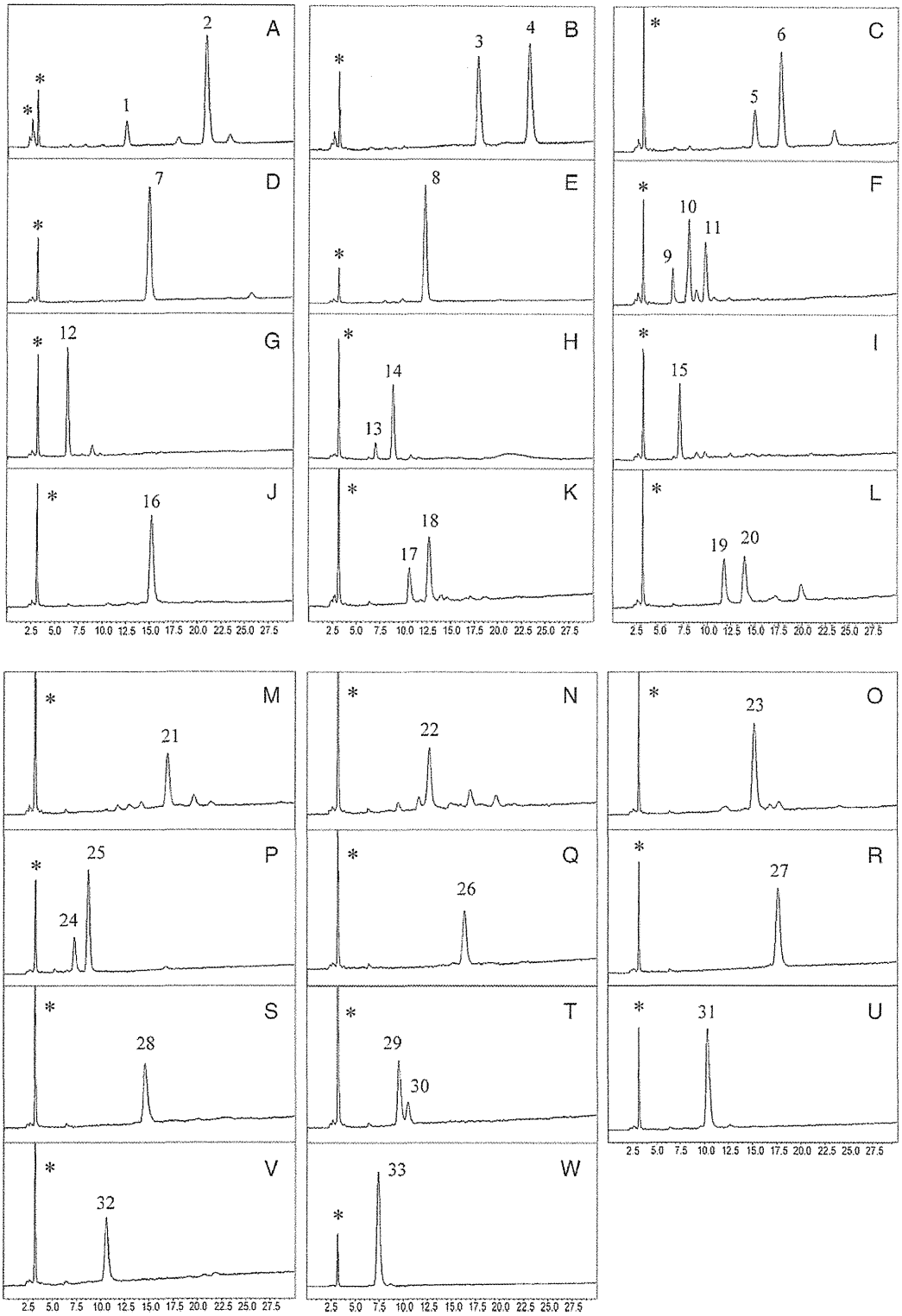

Fig. 3. Amide column elution profiles of PA-glycans of pig islets from each different fraction separated on the ODS column. (**A**) ODS peak-N1 + N5′. Peak 1 is the epimerization of the ODS peak-N5. Peak 2 was then settled as N1. (**B**) ODS peak-N2. Peaks 3 and 4 correspond to N2-1 and N2-2, respectively. (**C**) ODS peak-N3. Peak 5 was contamination of the ODS peak-N4. Peak 6 corresponds to N3. (**D**) ODS peak-N4. Peak 7 corresponds to N4. (**E**) ODS peak-N5. Peak 8 corresponds to N5. (**F**) ODS peak-N6. Peak 9 was contamination of ODS peak-N7. Peaks 10 and 11 correspond to N6-1 and N6-2, respectively. (**G**) ODS peak-N7. Peak 12 corresponds to N7. (**H**) ODS peak-N8. Peak 13 was contamination of ODS peak-N9. Peak 14 corresponds to N8. (**I**) ODS peak-N9. Peak 15 corresponds to N9. (**J**) ODS peak-M1.

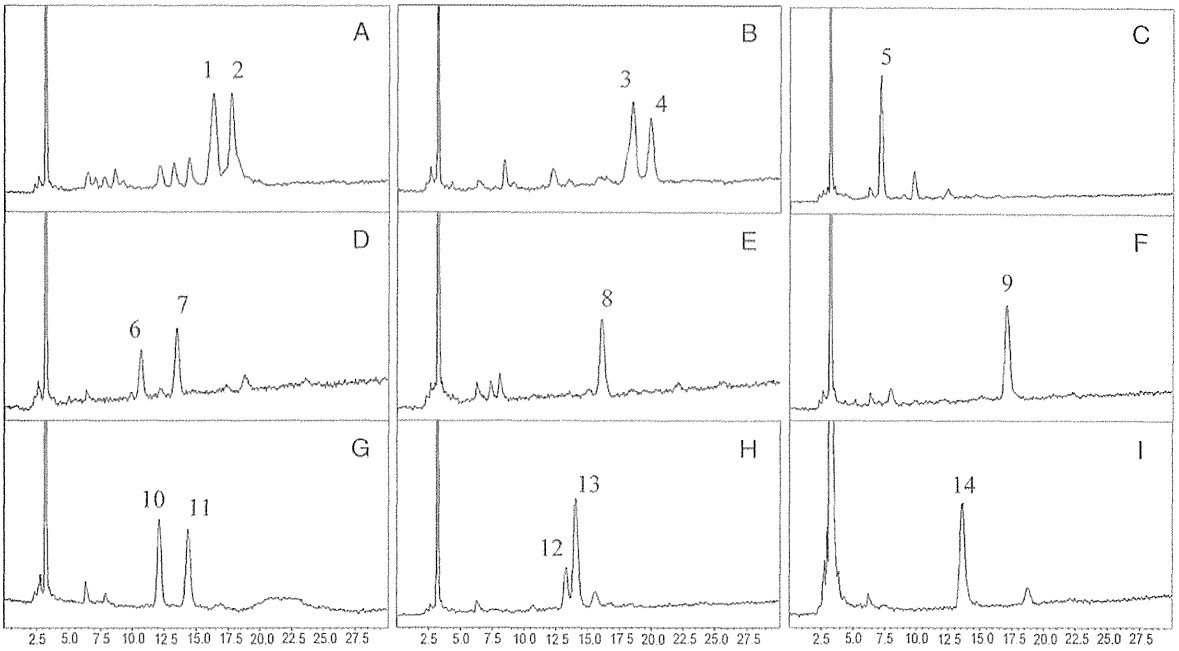

Fig. 4. Amide column elution profiles of PA-glycans from each fraction separated on the ODS column of human islets. (**A**) ODS peak-N5. Peaks 1 and 2 correspond to N5-1 and N5-2, respectively. (**B**) ODS peak-N6. Peaks 3 and 4 correspond to N6-1 and N6-2, respectively. (**C**) ODS peak-N11. Peak 5 corresponds to N11. (**D**) ODS peak-N12. Peaks 6 and 7 correspond to N12-1 and N12-2, respectively. (**E**) ODS peak-N13. Peak 8 corresponds to N13. (**F**) ODS peak-M1. Peak 9 corresponds to M1. (**G**) ODS peak-M2. Peaks 10 and 11 correspond to M2-1 and M2-2, respectively. (**H**) ODS peak-M4. Peaks 12 and 13 correspond to M4-1 and M4-2, respectively. (**I**) ODS peak-D2. Peak 14 corresponds to D2.

No terminal fucose was detected in the *N*-glycans from either type of islets in this study.

Previous studies reported by other groups concluded that many kinds of *N*-glycans are found in API, using MALDI-TOF/MS and MS/MS (Kim, Gil et al. 2008; Kim, Gil et al. 2009; Kim, Harvey et al. 2009). The difference in the number of detected *N*-glycans in this study can be attributed to the sensitivity of the MS method and HPLC. It, thus, appears that the accuracy of the data presented here using HPLC mapping in conjunction with a MALDI-TOF technique provided much more detailed information. That is, MS data are sensitive and can be rapidly obtained, but indicate only a glycan structure based on the calculated molecular weight. Therefore, discriminating between isomeric structures becomes difficult (Wheeler and Harvey 2001). In addition, except for N-glycolylneuraminic acid (NeuGc), it does not indicate the specific structure of sialyl acids present. On the other hand, the data reported herein can be used to identify the representative features of each *N*-glycan in the API preparation. However, the possibility that several glycans, such as pN6-2, pM2-1, pM2-2, pM3-1, pM3-2 and pM5, that were not detected in humans islets as major *N*-glycans are expressed in human islets at very low levels cannot be completely excluded. In addition, concerning the sulfated *N*-glycans such as S1-1, S1-2, S2, MS1 and MS3, the accuracy in identifying the position of the SOH3 attached to β1-4GalNAc was not clear in this study, and it is possible that these sulfated glycans also may be produced in human islets or other tissues, because humans produce several sulfotransferase enzymes that can catalyze the attachment of a sulfate to GalNAc (Boregowda et al. 2005).

Chlorate is a selective inhibitor of adenosine triphosphate sulfate adenylyltransferase, the first enzyme in the sulfate activation pathway (Girard et al. 1998). It inhibits all sulfotransferases. Therefore, although API had a diminished antigenicity to human serum, especially IgM, as a result of the presence of sodium chlorate treatment, a structural analysis of the changes on the sulfated *N*-glycans and other nonsulfated glycans of the API after the treatment might be needed to assess antigenicity issues. On the other hand, it was not possible to determine the binding site of the sulfate residue to GalNAc using this method. However, the possibility that the sulfate residue is one of the non-Gal antigens in pig islets cannot be excluded based on the data presented herein. Further study will be needed to analyze the non-Gal antigen in pig islets, especially to sulfotransferase enzymes.

In comparison with a report concerning the pig lung and trachea, using exactly the same HPLC mapping in conjunction with the MALDI-TOF technique, Sriwilaijaroen et al. (2011) reported a relatively small percent of high-mannose type

Peak 16 corresponds to M1. (**K**) ODS peak-M2. Peaks 17 and 18 correspond to M2-1 and M2-2, respectively. (**L**) ODS peak-M3. Peaks 19 and 20 correspond to M3-1 and M3-2, respectively. (**M**) ODS peak-M4. Peak 21 corresponds to M4. **N**: ODS peak-M5. Peak 22 corresponds to M5. (**O**) ODS peak-M6. Peak 23 corresponds to M6. (**P**) ODS peak-S1. Peaks 24 and 25 were identified as S1-1 and S1-2, respectively. (**Q**): ODS peak-D1. Peak 26 corresponds to D1. (**R**) ODS peak-D2. Peak 27 corresponds to D2. (**S**) ODS peak-D3. Peak 28 corresponds to D3. (**T**) ODS peak-MS1. Peak 29 corresponds to MS1. Peak 30 is the epimerization of ODS peak-MS2. (**U**) ODS peak-MS2. Peak 31 corresponds to MS2. (**V**) ODS peak-MS3. Peak 32 corresponds to MS3. (**W**) ODS peak-S2. Peak 33 corresponds to S2. *Not a sugar.

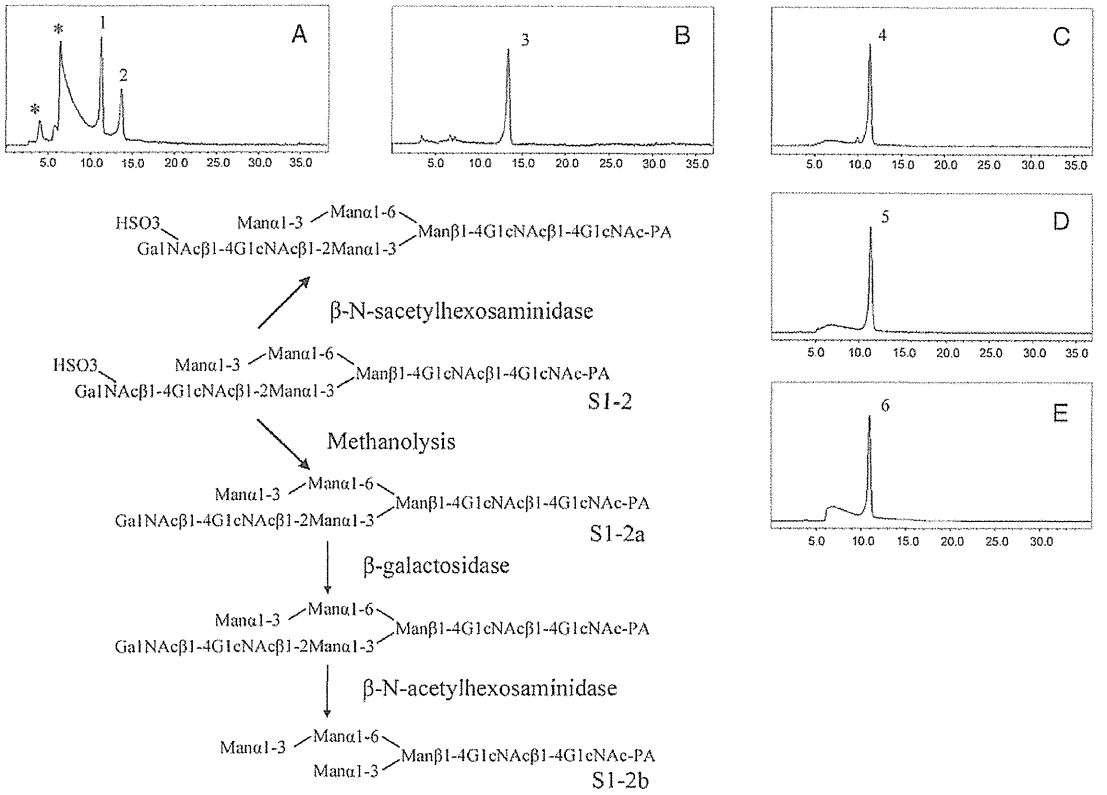

Fig. 5. Structural analysis of S1-2. (**A**) ODS peak after methanolysis treatment of S1-2. Peak 1 is the nonreacted sample, S1-2 (7.5 GU and 1641 Da). Peak 2 corresponds to S1-2a (8.3 GU and 1557 Da). (**B**) ODS peak after β-galactosidase treatment to S1-2a. Peak 3 is identical to S1-2a in ODS (GU) and molecular weight. (**C**) ODS peak after β-*N*-acetylhexosaminidase treatment of S1-2a. Peak 4 corresponds to S1-2b (7.5 GU and 1151 Da). (**D**) ODS peak after co-chromatography of S1-2b and M4.1. S1-2b was then proved to be the same structure as M4.1 in GALAXY. (**E**) ODS peak after β-galactosidase treatment to S1-2. Peak 6 is just the same as S1-2 in GU and molecular weight. * Not a sugar.

N-glycans. However, in this study, pig islets contain a relatively large percent of *N*-glycans, 81%, and human islets also contain 76.7%. Therefore, this evidence related to high-mannose types was assumed to be a typical feature of islets. It is noteworthy that in this pig islets study no evidence was found for the presence of α-Gal and NeuGc structures, while the pig lung and trachea clearly produce both antigens. Concerning α-Gal, as has been indicated in many reports, pig islets express very low levels of α-Gal. On the other hand, concerning NeuGc, our previous study reported that NeuGc is expressed on the *N*-glycans of API (Komoda et al. 2004). Therefore, pig islets must contain NeuGc in relatively minor amounts and, as a result, were not detected in this study, because pig lung and trachea contain relatively minor levels of NeuGc structures.

In addition, NeuGc-Gal-GlcNAc and Galα1-3 Lewis x (Lew^x) were recently reported as novel antigens, as evidenced by a structural analysis of *N*-glycans from the miniature pig kidney (Kim et al. 2006). However, neither of these antigens was detected in this study.

Blixt et al. (2009) reported on the carbohydrate specificities of sera obtained from clinical patients in whom neonatal bone pig islet-like cell clusters (NPCC) had been intraportally injected, using a printed covalent glycan array with 200 structurally defined glycans. Besides α-Gal and NeuGc, the patients had Abs against terminal α-linked GalNAc, β3-linked Gal especially Galβ1,3GlcNAc even if terminally sulfated or sialylated, β-GlcNAc except for β1,3-linked, oligomannosyl compounds, some neuranimic acid (NeuAc) and Galα1-3Lew^x. Compared with the data reported here, pM5 has β-GlcNAc, might be applicable for the target structure of the patients. In addition, N6-2, pM2-2 and pM3-2, which contain Manα1-3Manα1-6Man structures, are also potential target antigens. However, the antigenicity of NPCC may slightly be different from that for API.

As the other non-Gal antigens, the Forssman, the terminal GalNAc related to the Tn-antigen (GalNAcα-*O*-Ser/Thr), T-antigen (Thomsen-Friedenreich; Galβ1,3GalNAcα-*O*-Ser/Thr) and sialyl-Tn antigen (NeuAcα2,6GalNAcα-*O*-Ser/Thr) are also reported to be important (Ezzelarab et al. 2005). However, these glycans are related to *O*-glycans and glicolipids (Diswall et al. 2011).

In summary, as a feature, pig islets are rich in high-mannose type *N*-glycans, especially relatively low amounts of mannose. Several API structures, such as N6-2, pM2-1, 2-2, 3-1, 3-2, and pM5, and the sulfate structure, β-linked GalNAc-SOH3, were not detected in human islets. In addition, it is possible that the sulfated glycans of API are involved in the observed antigenicity to human serum. The data herein provide important information that can be useful to future clinical xenotransplantation studies.

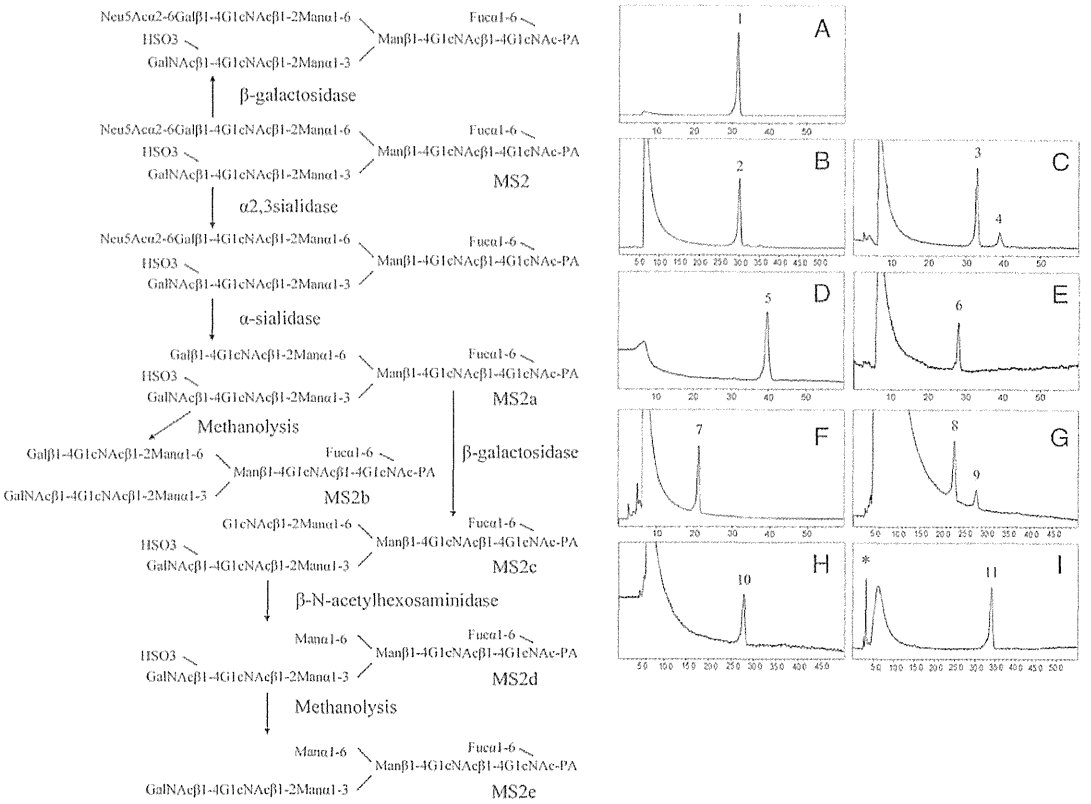

Fig. 6. Structural analysis of MS2. (**A**) ODS peak after α2,3-sialidase treatment to MS2. Peak 1 was just the same as MS2 in GU and molecular weight. (**B**) ODS peak after α-sialidase treatment to MS2. Peak 2 corresponds to MS2a (12.1 GU and 1988 Da). (**C**) ODS peak after methanolysis treatment to MS2a. Peak 3 is the nonreacted sample. Peak 4 lacked one sulfate residue from MS2a and corresponds to MS2b (13.9 GU and 1907 Da). (**D**) ODS peak after co-chromatography of MS2b and 210.4a in GALAXY. MS2b was proved to be the same structure as the 210.4a in GALAXY. (**E**) ODS peak after β-galactisidase treatment to MS2a. Peak 6 lacked one galactose from MS2a and corresponds to MS2c (11.4 GU and 1826 Da). (**F**) ODS peak after β-*N*-acetylhexosaminidase treatment to MS2c. Peak 7 corresponds to MS2d (9.7 GU and 1622 Da). (**G**) ODS peak after methanolysis treatment of MS2d. Peak 8 was the nonreacted sample. Peak 9 lacked one sulfate residue from MS2d and corresponds to MS2e (11.0 GU and 1541 Da). (**H**) ODS peak after co-chromatography of MS2e and 110.4a in GALAXY. MS2e was proved to be the same structure as the 110.4a in GALAXY. (**I**) ODS peak after β-galactisidase treatment to MS2. Peak 11 is identical to MS2 in GU and molecular weight. * Not a sugar.

Materials and methods

Pig islet isolation

Pancreatic glands were removed from several pigs at a slaughterhouse that handles young market weight pigs (Large White/Landrace x Duroc, 6 months old, ~100 kg). Isolation of porcine islets was performed using the Islet Isolation Technique (Goto et al. 2004), with minor modifications. Purified islet fractions were pooled and cultured at 37°C in a humidified atmosphere with 5% CO_2 in CMRL1066 medium (Biochrom, Berlin, Germany) supplemented with 20% heat inactivated porcine serum, 2 mm *N*-acetyl-L-alanyl-L-glutamine, 10 mM *N*-2-hydroxyethylpiperazine-*N*1-2-ethanesulfonic acid, 100 IU/mL penicillin, 100 μg/mL streptomycin (Biochrom) and 20 μg/mL ciprofloxacin (Bayer, Leverkusen, Germany).

Human islet isolation

The method used to isolate islets has been reported previously (Matsumoto et al. 2002). In brief, the pancreas was distended with a cold enzyme solution through the pancreatic duct using a pressure-controlled pump system. In all cases, the distended pancreata were digested using the semi-automated method (Matsumoto et al. 2006). All centrifuged pellets were collected in cold storage/purification stock solution (Mediatech, Inc., Manassas, VA).

Islet isolations were conducted based on the Edmonton protocol with our modifications. The results of the isolations were evaluated based on the Edmonton protocol. Islets were purified with a COBE 2991 cell processor (CaridianBCT, Inc., Lakewood, CO) using density-adjusted iodixanol-based continuous density gradient. The final preparation of islets was assessed using dithizone staining (Sigma Chemical Co., St. Louis, MO) for islet yield and purity. Islet yield was converted into a standard number of islet equivalents (diameter standardizing to 150 μm). Islet viability was evaluated with fluorescein diacetate (10 μmol/L) and propidium iodide (15 μmol/L) staining. All procedures were done at the Baylor Research Institute, TX.

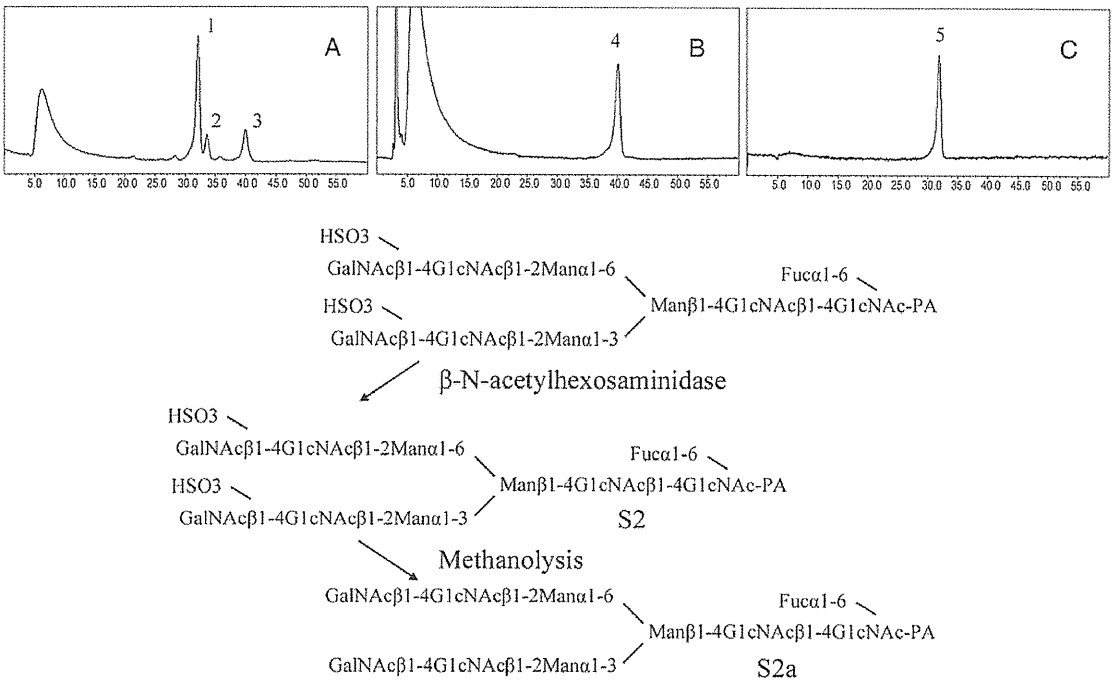

Fig. 7. Structural analysis of S2. (**A**) ODS peak after methanolysis treatment to S2. Peak 1 was the nonreacted sample, S2 (12.7 GU, 2110 Da). Peak 2 lacked one sulfate residue from S2, 13.2 GU and 2029 Da. Peak 2 lacked two sulfate residues from S2, corresponding to S2a (15.1 GU and 1948 Da). (**B**) ODS peak after co-chromatography of the samples of S2a and210.4b. S2a was the same structure as the 210.4b in GALAXY. (**C**) ODS peak after β-*N*-acetylhexosaminidase treatment of S2. Peak 5 was identical to S2 in GU and molecular weight.

Materials for analyses

Glycoamidase A from sweet almond, α-manosidase, β-galactosidase and β-*N*-acetylhexosaminidase from jack bean were purchased from Seikagaku Kogyo Co. (Tokyo, Japan). α-Gal from coffee bean was purchased from Oxford GlycoSciences, Inc. (Oxford, UK). Trypsin and chymotrypsin were obtained from Sigma (St. Louis, MO). Pronase protease from *Streptomyces griseus* was from Calbiochem (San Diego, CA). The PA derivatives of isomalto-oligosaccharides 4–20 (indicating the degree of polymerization of glucose residues) and reference PA-oligosaccharides were purchased from Seikagaku Kogyo Co.

Characterization of N*-glycan derived from islets*

The residue after extracting each islet with a chloroform–methanol solution was used as the starting material. All experimental procedures used, including the chromatographic conditions and glycosidase treatments, have been described previously (Takahashi et al. 2001). The extract was proteolyzed with chymotrypsin and trypsin mixture and further digested with glycoamidase A to release *N*-glycans. After the removal of the peptide materials, the reducing ends of the *N*-glycans were derivatized with 2-aminopyridine (Wako, Osaka, Japan). This mixture was applied to a DEAE column (Tosoh, Tokyo, Japan) or a TSK-gel Amide-80 column (Tosoh), and each fraction that was separated on the amide column was applied to a Shim-pack HRC-ODS column (Shimadzu, Kyoto, Japan). The elution times of the individual peaks onto the amide-silica and ODS columns were normalized with respect to a PA-derivatized isomalto-oligosaccharide with a known degree of polymerization, and are represented in units of glucose unit (GU). Thus, a given compound from these two columns provided a unique set of GU values, which corresponded to the coordinates of the two dimension HPLC map. The PA-oligosaccharides were identified by comparison with the coordinates of <500 reference PA-oligosaccharides in a homemade web application, GALAXY (http://www.glycoanalysis.info/) (Takahashi and Kato 2003). The calculated HPLC map based on the unit contribution values was used to estimate some high-mannose type PA-oligosaccharides. The PA-oligosaccharides were co-chromatographed with the reference to PA-oligosaccharides on the columns to confirm their identities.

MS analyses of PA-glycans

PA-oligosaccharides were subjected to MALDI-TOF-MS analysis. The matrix solution was prepared as follows: 10 mg of 2,5-dihydroxybenzoic acid (Sigma) was dissolved in 1:1 (v/v) of acetonitrile/water (1 mL). Stock solutions of PA-glycans were prepared by dissolving them in pure water. One microliter of sample solution was mixed on the target spot of a plate with 1 μL of matrix solution and then allowed to air-dry. MALDI-TOF-MS data were acquired in the positive modes using AXIMA-CFR (Shimadzu) operated in the linear mode.

Single islet cell preparation

Single-cell suspensions were prepared by the method described by Ono et al. (1977). Isolated islets were exposed to 0.04% ethylenediaminetetraacetic acid for 5 min at room temperature

Table I. Structures and relative quantities of neutral, mono-sialyl, di-sialyl or mono-sulfate, mono-sialyl-mono-sulfate and di-sulfate PA-oligosaccharides derived from human and porcine islets

Peak code number	GU[a] ODS (Amid)	Molecular[b] mass (Da)	Structure[c]	Relative quantity (%)[d]	
				Pig	
Neutral glycan					
N1	4.9 (8.8)	1800	Man α 1–2Man α 1–6 Man α 1–6 Man α 1–3 Man β 1–4GlcNAc β 1–4GlcNAc–PA Man α 1–2Man α 1–2Man α 1–3	11.6	24.9
N2-1	5.3 (7.9)	1638	Man α 1–2Man α 1–6 Man α 1–6 Man α 1–3 Man β 1–4GlcNAc β 1–4GlcNAc–PA Man α 1–2Man α 1–3	5.8	3.5
N2-2	5.3 (9.5)	1962	Man α 1–2Man α 1–6 Man α 1–6 Man α 1–2Man α 1–3 Man β 1–4GlcNAc β 1–4GlcNAc–PA Man α 1–2Man α 1–2Man α 1–3	7.4	9.5
N3	6.0 (7.9)	1638	Man α 1–6 Man α 1–6 Man α 1–3 Man β 1–4GlcNAc β 1–4GlcNAc–PA Man α 1–2Man α 1–2Man α 1–3	3.0	1.9
N4	6.2 (7.0)	1475	Man α 1–6 Man α 1–6 Man α 1–3 Man β 1–4GlcNAc β 1–4GlcNAc–PA Man α 1–2Man α 1–2Man α 1–3	16.7	10.1
pN5 = hN7	7.3 (6.1)	1313	Man α 1–6 Man α 1–6 Man α 1–3 Man β 1–4GlcNAc β 1–4GlcNAc–PA Man α 1–3	24.0	11.3
pN6-1 = hN8	7.5 (4.2)	989	Man α 1–6 Man β 1–4GlcNAc β 1–4GlcNAc–PA Man α 1–3	2.3	6.2

Continued

Table I. (Continued)

Peak code number	GU[a] ODS (Amid)	Molecular[b] mass (Da)	Structure[c]	Relative quantity (%)[d]	
				Pig	
pN6-2	7.5 (5.1)	1151	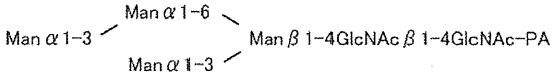	1.7	-
pN7 = hN9	7.7 (3.3)	827	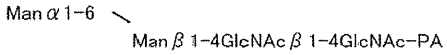	2.4	2.2
pN8 = hN10	10.3 (4.6)	1135	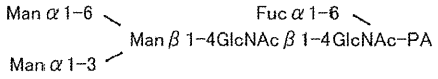	3.9	4.1
pN9 = hN11	10.5 (3.7)	973	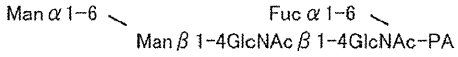	2.2	3.0
hN12-1	12.8 (5.4)	1541	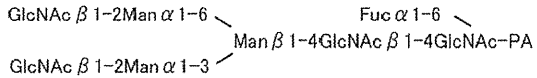	–	1.8
hN12-2	12.8 (6.5)	1948	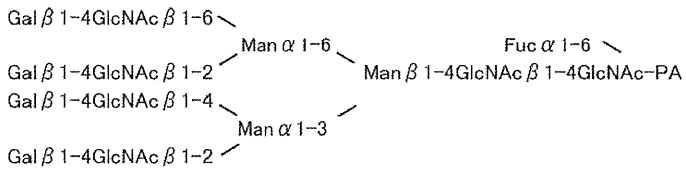	–	2.9
hN13	14.2 (7.4)	1866	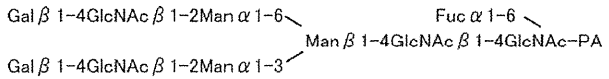	–	3.1
hN5-1	6.6 (7.4)	1558	(Hexose)4(HexNAc)4(PA)1[e]	–	2.7
hN5-2	6.6 (7.9)	1720	(Hexose)5(HexNAc)4(PA)1[e]	–	2.0
hN6-1	6.9 (8.1)	1720	(Hexose)5(HexNAc)4(PA)1[e]	–	1.5
hN6-2	6.9 (8.5)	1882	(Hexose)6(HexNAc)4(PA)1[e]	–	1.2

[a]Units of GU were calculated from the elution times of the peaks obtained from the ODS column in Figure 2 and the Amide column in Figure 3.
[b]Average mass calculated from the *m/z* values of $[M + Na]^+$ or $[M + H]^+$ion for neural, $[M - H]^-$ ion for mono-sialyl and mono-sulfated and $[M + Na - 2H]^-$ ions for mono-sialyl-mono-sulfated and di-sulfated PA-oligosaccharides (Supplementary data, Figure S1).
[c]Structures of PA-oligosaccharides are represented.
[d]Molecular percentage of was calculated from the peak area in Figure 2 by comparison with total *N*-glycan content in each islet tissue.
[e]*N*-glycans did not coincide with those of known references in the GALAXY database.